Global and Planetary Change 157 (2017) 93–113

Contents lists available at ScienceDirect

Global and Planetary Change

journal homepage: www.elsevier.com/locate/gloplacha

Invited review article

Impacts of the dam-orientated water-sediment regulation scheme on the lower reaches and delta of the Yellow River (Huanghe): A review

Houjie Wang[a,b,*], Xiao Wu[a,b], Naishuang Bi[a,b], Song Li[c], Ping Yuan[a], Aimei Wang[a], James P.M. Syvitski[d], Yoshiki Saito[e,f], Zuosheng Yang[a], Sumei Liu[g], Jeffrey Nittrouer[h]

[a] College of Marine Geosciences, Key Laboratory of Submarine Geosciences and Prospecting Techniques, Ocean University of China, 238 Songling Rd., Qingdao 266100, China
[b] Laboratory for Marine Geology, Qingdao National Laboratory for Marine Science and Technology, Qingdao 266061, China
[c] Department of Oceanography and Coastal Sciences, Louisiana State University, Baton Rouge, LA 70803, USA
[d] Community Surface Dynamics Modeling System, INSTAAR, University of Colorado, Boulder, CO 80309-0545, USA
[e] Geological Survey of Japan, National Institute of Advanced Industrial Science and Technology (AIST), Central 7, Higashi 1-1-1, Tsukuba, Ibaraki 305-8567, Japan
[f] Estuary Research Center, Shimane University, 1060, Nishikawatsu-cho, Matsue, Shimane 690-8504, Japan
[g] Key Laboratory of Marine Chemistry Theory and Technology, Ministry of Education, China, 238 Songling Rd., Qingdao 266100, China
[h] Department of Earth Science, Rice University, 6100 Main Street, Houston, TX 77005, USA

ARTICLE INFO

Keywords:
Water-sediment regulation
The Yellow River
Human activity
Delta morphology
Coastal ecosystem

ABSTRACT

The water-sediment regulation scheme (WSRS), beginning in 2002, is an unprecedented engineering effort to manage the Yellow River with the aims to mitigate the siltation both in the lower river channel and within the Xiaolangdi Reservoir utilizing the dam-regulated flood water. Ten years after its initial implementation, multi-disciplinary indicators allow us to offer a comprehensive review of this human intervention on a river-coastal system. The WSRS generally achieved its objective, including bed erosion in the lower reaches with increasing capacity for flood discharge and the mitigation of reservoir siltation. However, the WSRS presented unexpected disturbances on the delta and coastal system. Increasing grain size of suspended sediment and decreasing suspended sediment concentration at the river mouth resulted in a regime shift of sediment transport patterns that enhanced the disequilibrium of the delta. The WSRS induced an impulse delivery of nutrients and pollutants within a short period (~20 days), which together with the altered hydrological cycle, impacted the estuarine and coastal ecosystem. We expect that the sediment yield from the loess region in the future will decrease due to soil-conservation practices, and the lower channel erosion will also decrease as the riverbed armors with coarser sediment. These, in combination with uncertain water discharge concomitant with climate change, increasing water demands and delta subsidence, will put the delta and coastal ocean at high environmental risks. In the context of global change, this work depicts a scenario of human impacts in the river basin that were transferred along the hydrological pathway to the coastal system and remotely transformed the different components of coastal environment. The synthesis review of the WSRS indicates that an integrated management of the river-coast continuum is crucially important for the sustainability of the entire river-delta system. The lessons learned from the WSRS in the Yellow River provide insights to the integrated management of large rivers worldwide.

1. Introduction

Given the central importance of water to human society, the hydrological cycle, as well as the relevant delivery of terrestrial materials, has been one of the most impacted components of the earth system (Steffen et al., 2004). Human influence on the hydrological cycle, starting ~4000 years ago, however, has been sharply intensified at an accelerating rate since the 20th century and become a dominant forcing that appears to be competitive to the natural forces over the last 60 years (Meybeck and Vörösmarty, 2005; Syvitski and Kettner, 2011; Yang et al., 2015). Rivers play a primary role in the global hydrological cycle by collecting run-off from precipitation and moving it back towards the oceans, and in influencing global biogeochemical cycles with their delivery to the ocean of ~20 billion tonnes of terrestrial sediment per year (Gt/yr, 10^9 tonnes/yr), prior to significant dam interception, and ~0.37 Gt/yr of terrestrial organic carbon (Milliman and Meade, 1983; Milliman and Syvitski, 1992; Syvitski et al., 2005; Seitzinger et al., 2005; Dai et al., 2012).

* Corresponding author at: College of Marine Geosciences, Ocean University of China, 238 Songling Rd., Qingdao 266100, China.
E-mail address: hjwang@mail.ouc.edu.cn (H. Wang).

http://dx.doi.org/10.1016/j.gloplacha.2017.08.005
Received 23 September 2016; Received in revised form 7 August 2017; Accepted 8 August 2017
Available online 09 August 2017
0921-8181/

Human activities that impact the river system include dams and reservoirs, flow diversions and water extractions. By far > 45,000 dams over 15 m in height have been registered in the world with the purpose of flood control and water extraction (Nilsson et al., 2005). These flourishing engineering works not only result in more water being stored on land and greater sedimentation behind these structures, but also by disconnecting rivers from their deltas. The dam regulation has decreased the sediment flux to the coastal ocean by ~5 Gt/yr by the 21st century (Syvitski and Kettner, 2011). During the past 50–70 years many sediment-starved deltas worldwide have been documented due to the rapid decreases in water and sediment discharging to the ocean; examples include the Mississippi (Meade and Parker, 1985) and Colorado (Schwarz et al., 1991) in America, Danube, Ebro, Po and Rhone (Walling and Fang, 2003; Syvitski and Saito, 2007; Syvitski and Kettner, 2007) in Europe, Yellow (Wang et al., 2006a, 2007), Yangtze (Yang et al., 2011a) and Mekong (Wang et al., 2011a) in Asia, and Nile (Stanley and Warne, 1998) in Africa.

Despite disputes among different stakeholders, construction of dams on large rivers mostly achieved their anticipated aims to regulate river discharge. However, dams have induced a series of environmental consequences that may or may not have been anticipated such as changes in aquatic ecosystem, reduction in sediment delivery to the ocean and significant delta erosion at global scale (Giosan et al., 2014; Yang et al., 2014). For example, the five large rivers in East and Southeast Asia (Yellow, Yangtze, Pearl, Red and Mekong) now collectively discharge ~600 million tonnes (Mt) of sediment to the sea every year, in contrast to ~2000 Mt/yr before the rivers were fragmented by dams (Wang et al., 2011a). Consequently, the reduction of sediment discharge to the sea, together with delta subsidence and sea-level rise put their deltas at high risks (Syvitski et al., 2009; Tessler et al., 2015).

1.1. The Yellow River Catchment

Among these human-altered river systems, the Yellow River (Huanghe) presents a typical example on how humans have battled this tameless river over thousands of years (Chen et al., 2012). The Yellow River was once the second largest river of the world in terms of sediment delivery to the sea, with a widely cited annual sediment load of 1.08 Gt/yr (Milliman and Meade, 1983). Originating from the eastern Qinghai–Tibet Plateau, the Yellow River drains a wide basin of > 75,000 km^2 with a total length of 5464 km (Wang et al., 2007; Fig. 1A). Nearly 90% of sediment is derived from its middle reaches where the loess deposits are extensive, whereas ~60% of river runoff is derived from the upper reaches. Given the nature of its huge sediment load but low water discharge (~49 km^3/yr, approximately 5% and 0.8% of those from Yangtze and Amazon, respectively) (Milliman and Meade, 1983), the Yellow River has been characterized by its high suspended sediment concentration (SSC) and catastrophic disasters to the Chinese nation over its long history (Chen et al., 2012). In the 2540 years prior to 1946, the Yellow River was extremely prone to frequent flooding and is believed to have flooded 1593 times, shifting its lower course 26 times with nine of them catastrophic in scale (Xu, 2003). In the middle reaches of the river across the Loess Plateau, many small tributaries with high sediment yields join the mainstream that is confined within a deep valley (Fig. 1B). The river's lower reaches offer a gentle slope downstream of Huayuankou (Figs. 1B and 2A; Wang et al., 2014a), where the sediment, particularly the coarser fraction, begins settling onto the riverbed. Consequently, the lower riverbed has been elevated due to siltation and the constraint of artificial levees (Chen et al., 2012). The natural and anthropogenic forces have resulted in riverbed higher than the surrounding areas by 5–8 m but lower than the river levees by only 3–5 m (Fig. 2B). The enhanced sediment yield from the loess region due to land-use changes from the growing populations since ~2000 years B.P. and the consequently elevated riverbed in the lower reaches caused catastrophic floods in the lower Yellow River, which forced the Chinese capital to move to South China in 1127 CE (Wang et al., 2007, 2014a). Management of the Yellow River and the flooding protections has been an intractable issue to governors of Chinese dynasties given the critical importance to societal and political stability (Chen et al., 2012).

1.2. The dam-orientated water-sediment regulation scheme (WSRS)

Since the 1950s, China has made great efforts on the Yellow River management, including the dam constructions in the upper and middle reaches (Fig. 1B), and the effective water-soil conservation program in the middle reaches since the 1970s in order to control the sediment yield in the loess region. The operation of large dams (e.g., Liujiaxia in 1968, Longyangxia in 1986 and Xiaolangdi in 1999, see Fig. 1B for locations) together with the land cover changes in the middle reaches have caused stepwise decreases in sediment delivery to the sea (Wang et al., 2007), and reduced the risk of flooding in the lower reaches. Yet the highly elevated riverbed and shallow channel in the lower reaches (Fig. 2) still threaten the livelihood of millions of people living in the fluvial plain. In addition, the Xiaolangdi Dam completed in 1999 with a reservoir storage capacity of 12.7 km^3, has faced serious siltation within its reservoir and a significant loss of effective storage capacity (Fig. 3). The reservoir storage capacity was reduced at a rate of 0.3 km^3/yr during the period of 1999–2007 (Fig. 3B). In 2002 the Yellow River Conservancy Committee (YRCC), as the official administrative department for the Yellow River, initiated the water-sediment regulation scheme (WSRS) as facilitated by the reservoirs of Xiaolangdi, Sanmenxia and Wanjiazhai (see Fig. 1B). The objectives of WSRS include scouring the lower riverbed to mitigate the siltation and expelling the sediment that previously accumulated within the reservoir to maintain the storage capacity by the dam-regulated artificial flood water (Wang et al., 2005). The WSRS has been implemented annually since 2002, usually lasting for ~20 days from mid-June to early July, and greatly altering the natural seasonal rhythm of the hydrological cycle, as ~30% and ~50% of annual water and sediment is discharged to the sea within a short period (Table 1). Such an impulsive discharge of water and sediment has impacts on the coastal ocean including regime shift of sediment dynamics, changes in quality of wetlands and nutrient delivery - all closely associated with the health of the coastal ecosystem.

Wang et al. (2005) reported the instability of the estuarine plume pathway during the WSRS period mostly resulting from the rapidly changing bathymetry at the river mouth because of deposition of coarser sediment derived from the lower riverbed. Wang et al. (2010a) proposed that the WSRS-induced increase in grain size of suspended sediment to the sea had significant impacts on the morphology of the river mouth since a larger portion of sediment would rapidly deposit at the active river mouth and contribute to river mouth accretion. Bi et al. (2014a) confirmed that the present river mouth accreted at a rate of ~4 km^2/yr since 2002 in contrast with 0.01 km^2/yr for the period of 1996–2002, even though the average annual sediment load to the sea since 2002 was 0.17 Gt/yr, almost the same as during the period of 1996–2002 (~0.16 Gt/yr). Therefore, the coarser sediment derived from the lower channel erosion during WSRS played an important role in influencing the river mouth morphology (Wu et al., 2017). In addition, WSRS had important influences on the estuarine biogeochemical cycles. Zhang et al. (2013) reported that ~35% and 56% of the annual dissolved organic carbon (DOC) and particulate organic carbon (POC) were discharged to the sea during WSRS, respectively. Nutrient fluxes from the Yellow River to the Bohai Sea during the WSRS period increased to be 8–10 times of those during the non-WSRS period. In addition, nutrient imbalance was aggravated during the WSRS, which most likely presents significant impacts on the coastal ecosystem (Liu et al., 2012). Besides the rapid exports of carbon and nutrients, heavy metals such as lead (Pb) and zinc (Zn), and pollutants such as polycyclic aromatic hydrocarbon (PAH) were also flushed to the sea during the WSRS either from the crop lands in lower reaches or directly from the reservoir (Bi et al., 2014b; Dong et al., 2015). Consequently, soils in

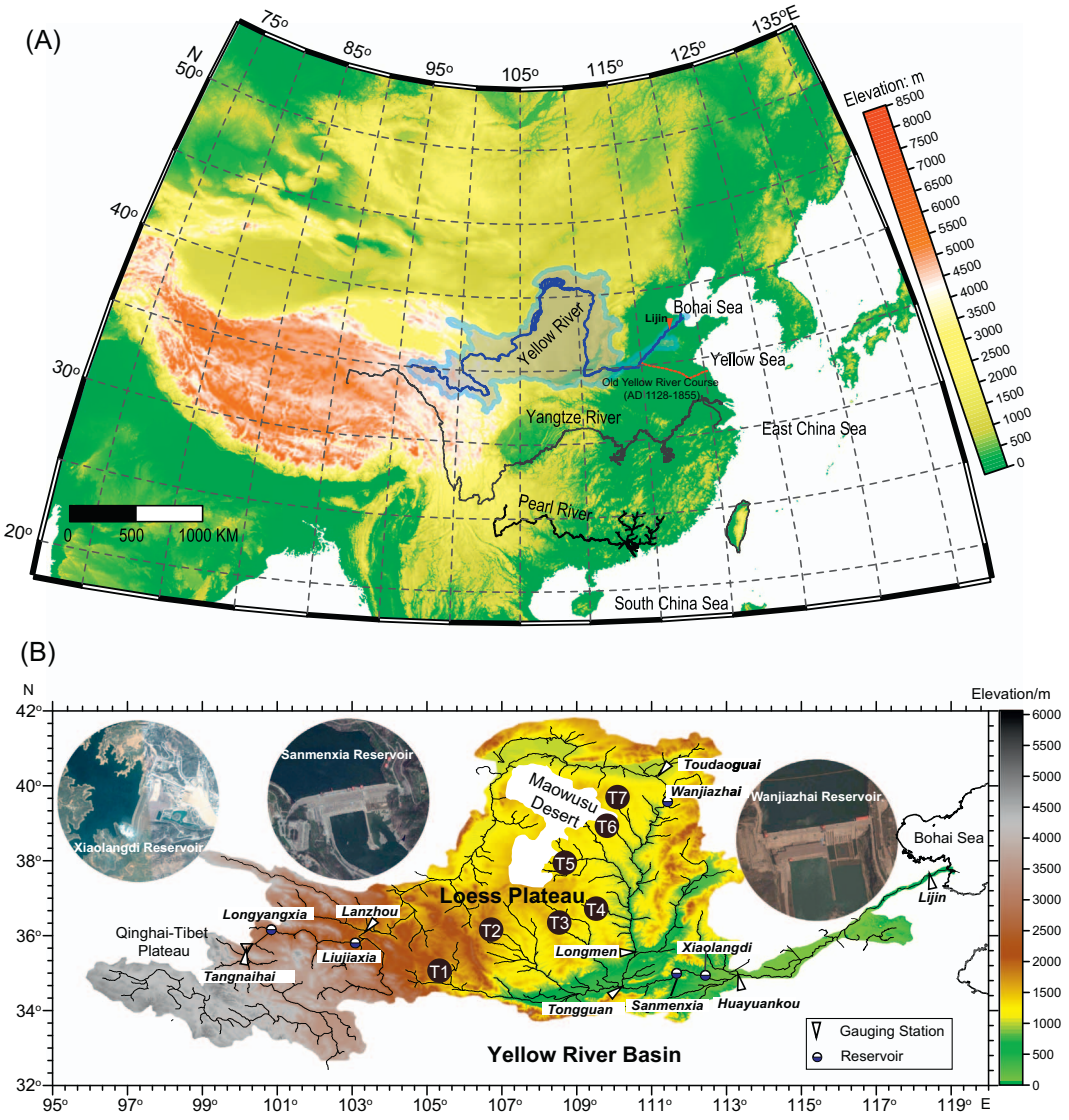

Fig. 1. Location of the Yellow River in China (A), and map of the Yellow River Basin with the locations of major reservoirs and gauging stations (B). The basin relief was derived from SRTM (Shuttle Radar Topography Mission) datasets, available at http://srtm.usgs.gov/index.php. The dashed red line in Panel (A) indicates the old Yellow River course during 1128–1885 CE when the Yellow River entered the Yellow Sea. The pictures of Wanjiazhai, Sanmenxia and Xiaolangdi that jointly operated to implement the water-sediment regulation scheme were acquired from Google Earth. Major tributaries in the loess region are: T1–Weihe River, T2–Jinghe River, T3–Beiluohe River, T4–Yanhe River, T5–Wudinghe River, T6–Kuyehe River and T7–Huangfuchuan River. (For interpretation of the references to colour in this figure legend, the reader is referred to the web version of this article.)

coastal wetlands around the river mouth were highly polluted after the WSRS (Bai et al., 2012), which degraded the quality of coastal wetland, even though the WSRS could quantitatively increase the wetland area.

The impacts of WSRS on the coastal ocean are diverse and profound. Ten years after its initial implementation, the existing multi-disciplinary datasets enable us to offer a comprehensive review of this human intervention on a river-coastal system. Here we present a synthesis review on how the short-period regulation impacted the different components of the river-coast continuum, and provide a perspective on the future changes. This would be a good example on how human activities impact the river hydrological process and biogeochemical cycle.

2. Data sources

The datasets we use include the long-term hydrographic records from major gauging stations of the Yellow River with temporal resolution ranging from day to year and annual data of median grain size of suspended sediment (Table 2). Since the 1950s the Yellow River has been well gauged; daily water discharge and SSC are recorded at major gauging stations along the mainstream.

Besides the hydrographic datasets released by the government agency (e.g., YRCC, Ministry of Water Resources of China, documents in Chinese are available at http://www.yellowriver.gov.cn/nishagonggao/), we analyzed the daily data of median grain size of suspended sediment at station Lijin from 2008 to 2010 from the published documents (e.g., Wei et al., 2011; Liu et al., 2012). Data of median grain size of surface sediment on the lower riverbed in 1999 and 2008 (Wan et al., 2013) were collected to show the changes in sediment size in the lower reaches induced by the WSRS (Table 2). Datasets of channel erosion in different river segments downstream the Xiaolangdi Dam based on bathymetric surveys in the lower reaches (see Fig. 2A) from 2002 to 2013 were collected from Chen et al. (2009), Li et al. (2014) and Shang et al. (2015).

In order to clarify the impacts of WSRS on the morphology of the present river mouth, we collected the bathymetric data (1976–2012) at five cross-shore transects along the Yellow River Delta from the YRCC, and used LANDSAT imagery from the United States Geological Survey

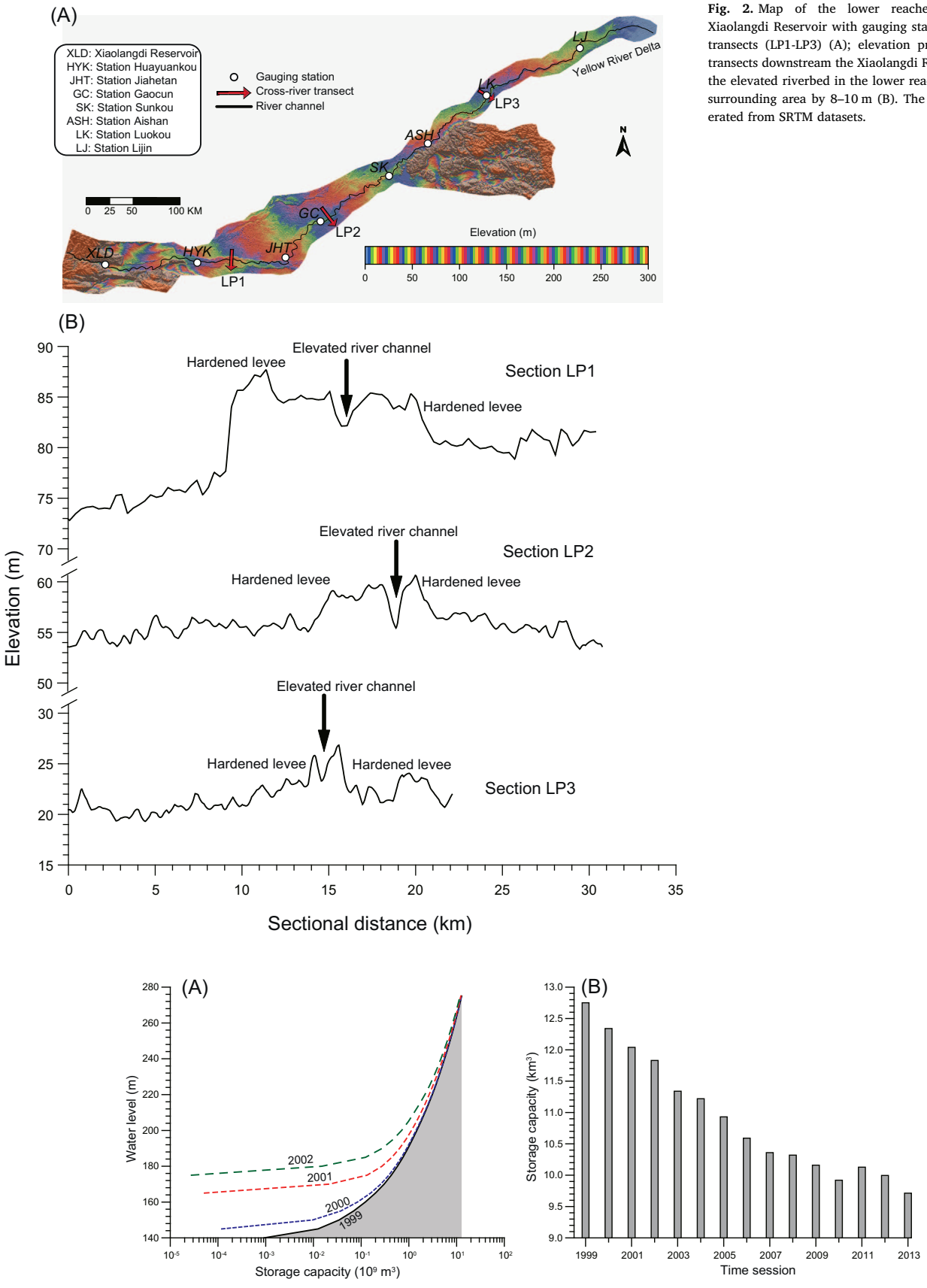

Fig. 2. Map of the lower reaches downstream the Xiaolangdi Reservoir with gauging stations and cross-river transects (LP1-LP3) (A); elevation profiles of cross-river transects downstream the Xiaolangdi Reservoir, illustrating the elevated riverbed in the lower reaches higher than the surrounding area by 8–10 m (B). The relief map was generated from SRTM datasets.

Fig. 3. Curves of reservoir water level vs. storage capacity from 1999 to 2002 (A); and annual variations of storage capacity of the Xiaolangdi Reservoir for a fixed water level of 275 m (B).

Table 1
Statistical information of water-sediment regulation from 2002 to 2013.

No.	Year	Starting	Ending	Max. Q (m^3/s)[a]	Max. SSC (kg/m^3)[b]	Water discharge to the sea		Sediment load to the sea	
						Q_w/(km^3)	Percentage (%)[c]	Qs/(Mt)	Percentage (%)[d]
1	2002	4-Jul	15-Jul	2360.0	25.2	2.3	55.4	51	93.0
2	2003	6-Sep	18-Sep	2590.0	77.6	2.8	14.6	121	32.2
3	2004	19-Jun	13-Jul	2870.0	19.9	5.0	25.3	78	28.6
4	2005	16-Jun	1-Jul	2780.0	21.9	3.7	17.9	56	30.0
5	2006	1-Jun	29-Jun	3590.0	18.0	5.1	26.6	65	44.0
6	2007[e]	19-Jun	7-Jul	3800.0	31.6	6.6	32.4	100	68.1
7		29-Jul	7-Aug	3630.0	34.3				
8	2008	19-Jun	3-Jul	3940.0	40.2	4.1	28.1	61	78.9
9	2009	19-Jun	8-Jul	3660.0	15.2	3.8	28.6	41	73.0
10	2010[f]	19-Jun	7-Jul	3520.0	64.2	8.5	44.0	137	81.9
11		24-Jul	3-Aug	3750.0	24.5				
12		15-Aug	21-Aug	2880.0	23.5				
13	2011	19-Jun	12-Jul	3110.0	34.6	3.9	21.1	43	46.7
14	2012	19-Jun	9-Jul	3470.0	34.4	4.8	17.0	64	35.0
15	2013	19-Jun	1-Jul	3570.0	24.6	5.4	22.8	60	34.6
Average				3301.0	32.6	4.7	27.8	73	53.8

[a] Maximum water flow at station Lijin.
[b] Maximum suspended sediment concentration at station Lijin.
[c] Water discharge during the WSRS in percentage of annual water discharge to the sea.
[d] Suspended sediment load during the WSRS in percentage of annual sediment load to the sea.
[e] Two WSRS events in 2007.
[f] Three WSRS events in 2010.

(http://glovis.usgs.gov/) for extracting the coastlines at different periods. In 2010, we collected samples of surface sediment at the present river mouth in May (before WSRS), July (during WSRS) and September (after WSRS) and analyzed the grain-size compositions in the laboratory to reveal the pattern of sediment dispersal and accumulation (Table 2). The datasets of nutrients and pollutants including the particulate organic carbon, particulate phosphate and lead absorbed by the sediment particle during WSRS are from Zhang et al. (2013), Liu et al. (2012) and Bi et al. (2014b). The datasets of autumn catches of Chinese Shrimp in the Bohai Sea as indicative to the changes of coastal ecosystem are from Deng and Zhuang (2001).

The complied datasets are diverse not only in their sources but also in spatial coverage and temporal range; the data allow us to present a synthesis understanding on how the river basin-coastal ocean system has been altered by the dam-orientated regulation over the past 10 years.

3. Results

3.1. Operation of the WSRS in the Yellow River

The Xiaolangdi Dam was completed in October 1999 with a height of 160 m and holding a reservoir with a storage capacity of 12.7 km^3 (Wang et al., 2006a). Given its critical geographic location (Figs. 1B and 2A), the Xiaolangdi Reservoir intercepted the water and sediment derived from the upper and middle reaches. Due to the high elevation of lower river channel, there is no tributary joining the mainstream as indicated by the high-resolution topographic imagery (Fig. 2A). Consequently, the regime of water and sediment in the lower reaches has been mostly dominated by the regulation of Xiaolangdi Reservoir since 2000 (Wang et al., 2011a).

In 2002 the YWCC began to implement the WSRS in early summer before the upcoming flooding season (July–September). The WSRS was designed to have two phases with different purposes (Fig. 4). During the first one (so-called water-regulation period) the clear water was

Table 2
Information of data sources.

Datasets	Description	Time range	Data source
Hydrographic data	Daily, monthly and annual water discharge and sediment load at station LJ	1950–2013	YRCC
	Monthly and annual water discharge and sediment load at station HYK	1950–2013	YRCC
	Annual water discharge and sediment load at station TG and from major tributaries in the middle reaches	1950–2013	YRCC
Grain size data	Annual median grain size at stations of TG, HYK and LJ	1960–2013	YRCC
	Daily grain size during WSRS in 2008, 2009 and 2010 at station LJ	2008–2010	Wei et al., 2011; Liu et al., 2012
	Median grain size of bed sediment along the lower reaches	1999/2008	Wan et al., 2013
Lower channel erosion	Erosion of segmented channel in the lower reaches due to WSRS	2002–2013	Chen et al., 2009; Li et al., 2014; Shang et al., 2015
Bathymetric data	Bathymetric data of five offshore transects along the Yellow River Delta	1976–2012	YRCC
LANDSAT data	LANDSAT imageries of the Qingshuigou delta lobe and shoreline changes	1996/2002/2015	USGS, http://glovis.usgs.gov/
	Shoreline of the Yellow River Delta derived from LANDSAT imageries	1976/1986/1996/2005	USGS, http://glovis.usgs.gov/
Surface sediment	Composition of surface sediments sampled off the present river mouth	May/July/September 2010	Wu et al., 2015a
Chemical data	Daily concentrations of particulate organic carbon (POC) and total phosphate during WSRS at station LJ	2008	Zhang et al., 2013
	Daily concentrations of particulate phosphorus (PP) and biogenic silica (BSi) during WSRS at station LJ	2009	Liu et al., 2012; Liu, 2015
	Daily lead (Pb) concentration during WSRS at station LJ	2009	Bi et al., 2014b

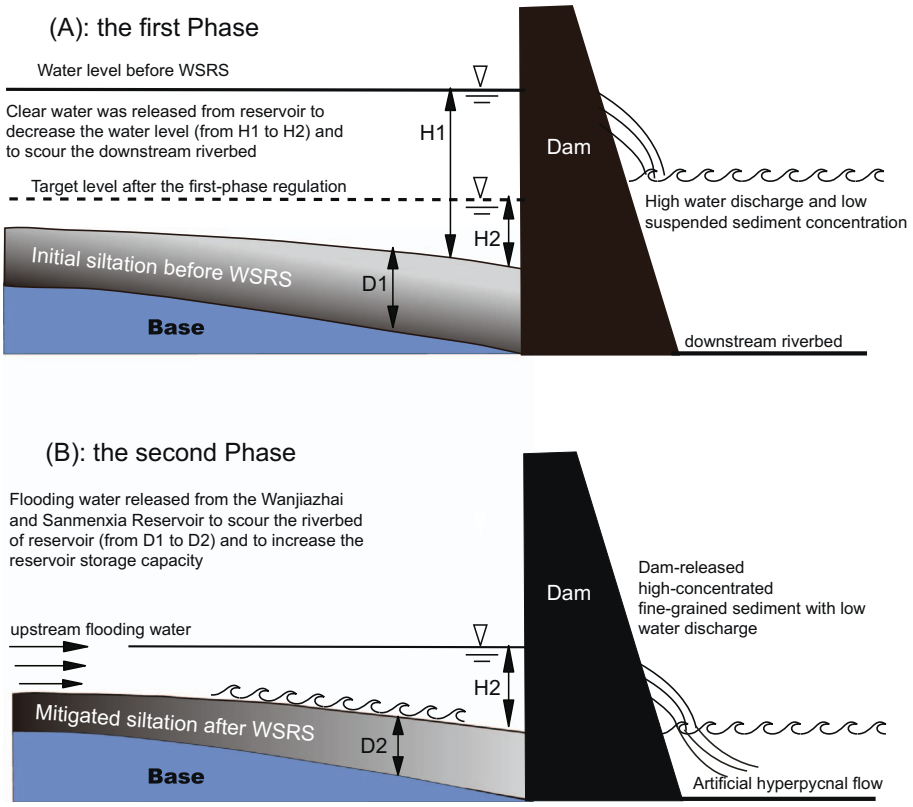

Fig. 4. Sketch diagram showing the two phases of WSRS. During the first phase (A), the water was released from the Xiaolangdi Reservoir in order to decrease the water level within the reservoir and to scour the riverbed in the lower reaches. During the second phase (B), the flooding water released from the Wanjiazhai and Sanmenxia Reservoir to scour the previously deposited sediment within the Xiaolangdi Reservoir and export the high-concentrated sediment to the lower reaches in a form of artificial hyperpycnal flow.

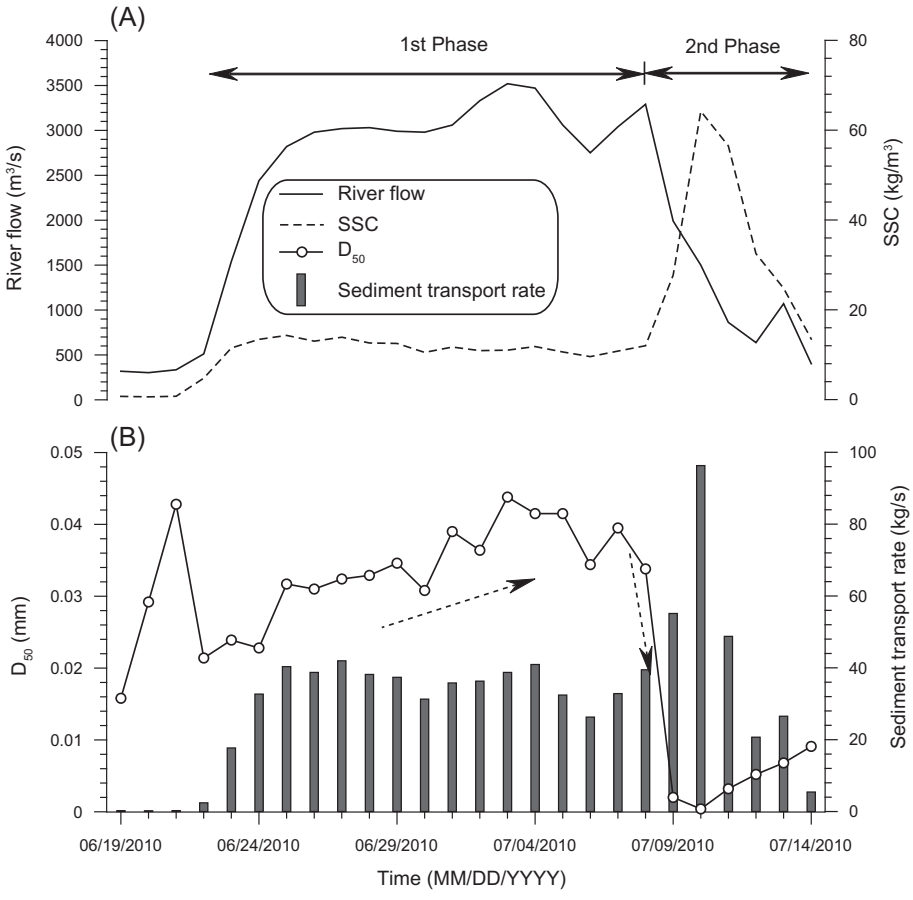

Fig. 5. Daily river flow, suspended sediment concentration (SSC) (A), median grain size of sediment (D_{50}) and sediment transport rate (B) at station Lijin during the WSRS in 2010.

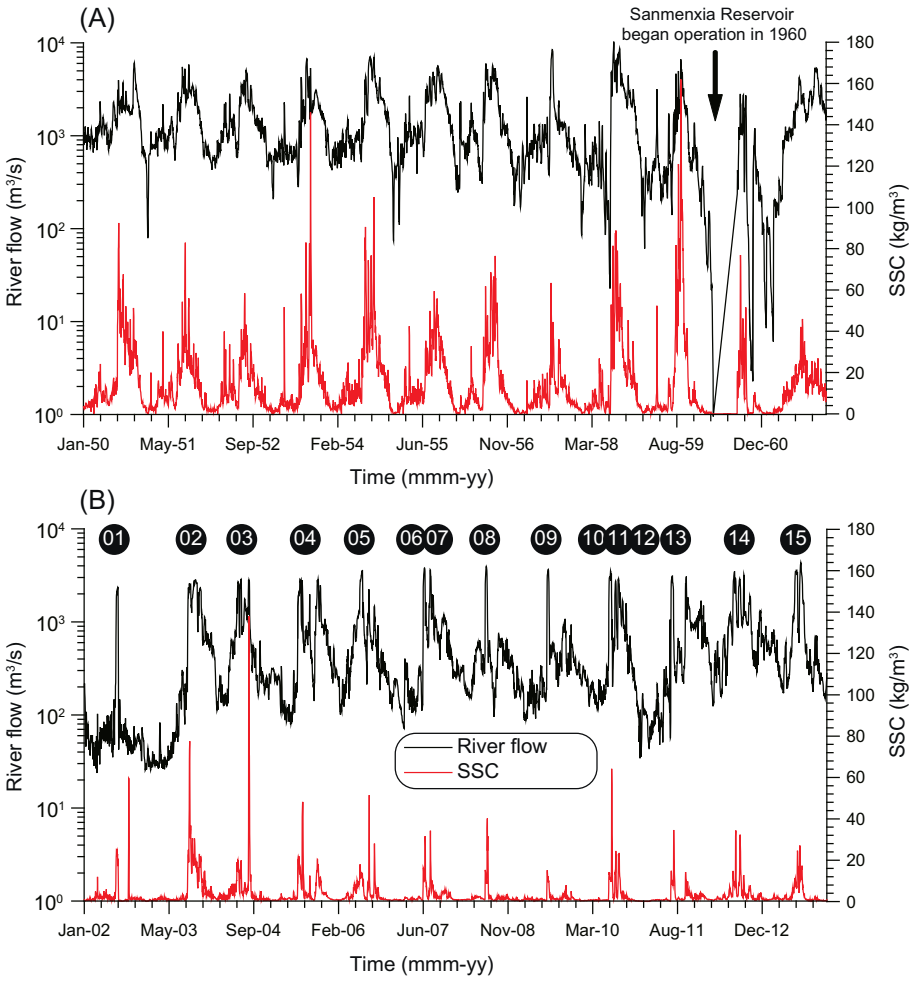

Fig. 6. Comparison of daily river flow and suspended sediment concentration recorded at station Lijin between 1950 and 1960 (A) and 2002–2013 (B), illustrating the episodic flooding events as regulated by the reservoirs since 2002. Totally 15 events of WSRS were implemented during 2002–2013 (see Table 1).

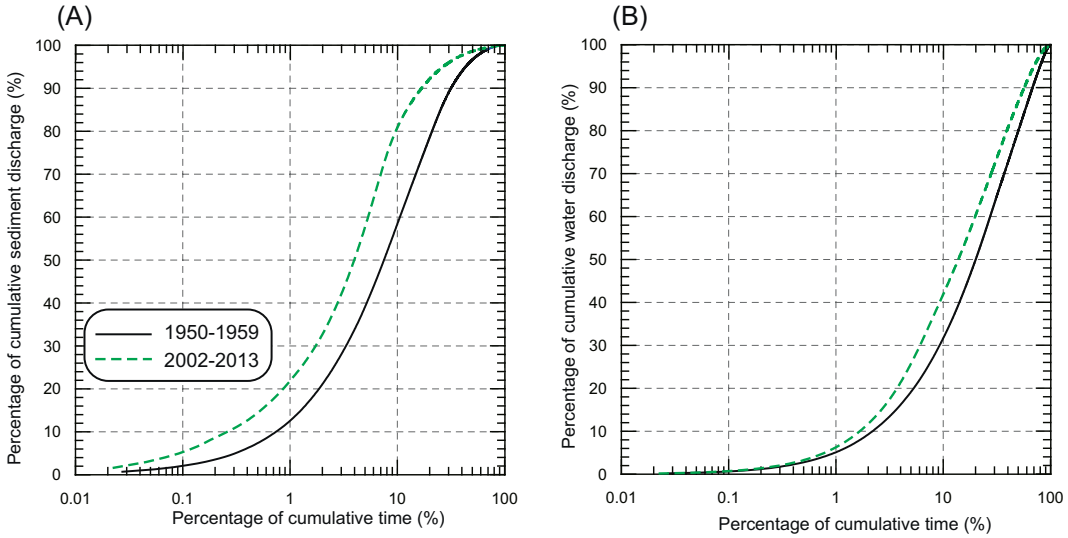

Fig. 7. Percentages of cumulative sediment discharge (A) and water discharge (B) to the sea vs. the percentage of cumulative time during the periods of 1950s and 2002–2013, respectively.

released from the reservoir in order to decrease the water level (Fig. 4A). The corresponding water flow increases rapidly from several hundreds of m^3/s to ~3000–3500 m^3/s within two days. The water-regulation usually lasts for ~10 days with maximum water discharge around 4000 m^3/s (Table 1) depending upon the initial water level within the reservoir, and contributes ~75% of total water discharge of WSRS to the lower reaches. Lower channel erosion thus became a dominant sediment source during the water-regulation period as the median grain size of suspended sediment delivered to the sea was approximately 0.035–0.04 mm (Wang et al., 2010a). During the second phase (so-called sediment-regulation period) the flooding water derived from the joint operation of upstream reservoirs (e.g. Sanmenxia

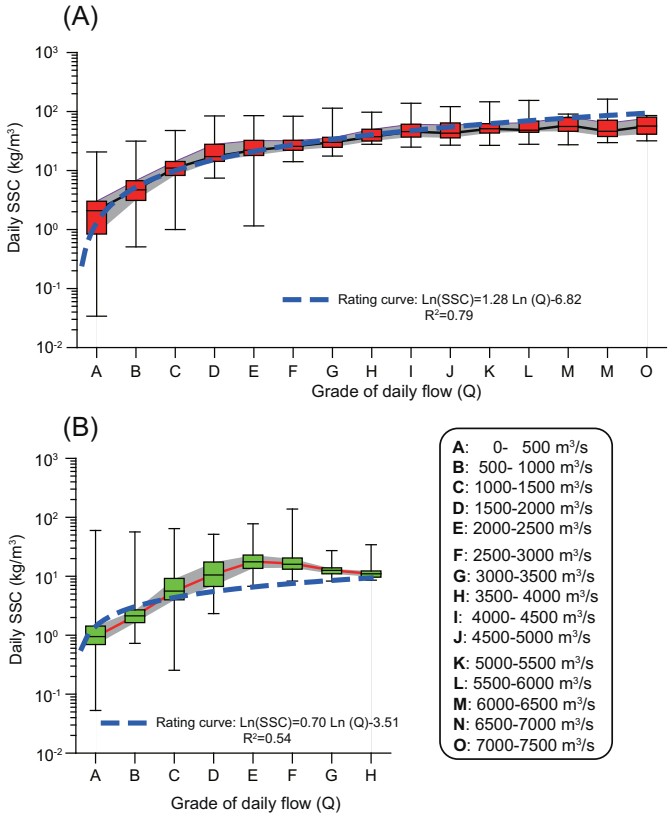

Fig. 8. Box-Whisker plots of daily SSC corresponding to different grades of daily river flow at station Lijin during the 1950s (A) and the period of 2002–2013 (B), indicating that the rating curve between daily SSC and daily water discharge was no longer applicable due to the impacts of WSRS.

Reservoir and Wanjiazhai Reservoir, see Fig.1B) is utilized to scour the sediment that previously accumulated within the Xiaolangdi Reservoir (Fig. 4B). The water discharge gradually decreases to ~2000–3000 m^3/s; however, the SSC increases rapidly to ~60–100 kg/m^3 within one day. As a result, sediment is exported from the reservoir as an artificial hyperpycnal flow with high sediment concentration and fluid density. The sediment-regulation usually lasts for 4–6 days, but is responsible for several to tens of million tonnes of sediment export from the Xiaolangdi Reservoir. As the WSRS is completed, the water discharge is controlled to be < 500 m^3/s, which represents a normal condition during the non-WSRS period.

During the second phase of regulation the sediment exported from the Xiaolangdi Reservoir is fine with a median grain size of ~0.006–0.010 mm, which renders the sediments delivered to the sea differ largely from those during the first phase, in terms of both sediment texture and sediment composition. The datasets we collected at the Lijin station during the WSRS in 2010 presented an example of sediment delivery to the sea that varied upon the different operations of reservoirs in the first and second phases (Fig. 5). The 2010 WSRS started on June 19 as the water discharge at station Lijin increased from 300 m^3/s to ~1500 m^3/s on June 23, with ~4 days in lag for flooding water travelling from Xiaolangdi to Lijin (Fig. 5A). Correspondingly, the SSC increased to ~12 kg/m^3 from ~0.7 kg/m^3 prior to WSRS. The high water discharge persisted for 16 days (the first phase), slightly fluctuating between 2500 m^3/s and 3500 m^3/s (Fig. 5A). From July 9 the water discharge began decreasing, whereas the SSC increased sharply to ~60 kg/m^3, approximately 85 and 5 times of values prior to the WSRS and during the first phase, respectively. During the first phase, the Xiaolangdi Reservoir released the clear water to scour the downstream riverbed; as a result, the corresponding median grain size on average was 0.034 mm from June 23 to July 8 (Fig. 5B). However, the fine-grained sediment export from the Xiaolangdi Reservoir during the second phase (July 9–14) drastically decreased the median grain size of suspended sediment at Lijin to be one order of magnitude lower than that during the first phase. The sediment flux, as calculated from the data of flow discharge and SSC (the bulk density of sediment used as 2.65 × 10^3 kg/m^3), indicated that the strong erosion of the lower riverbed derived ~49 Mt of coarse sediment delivered to the sea during the first phase (~16 days), whereas ~22 Mt of fine-grained sediment directly derived from the Xiaolangdi Reservoir was flushed to the sea during the second phase (~6 days) (Fig. 5B). Significant differences in sediment sources, median grain size and SSC between the two phases suggested important impacts of WSRS on the estuarine sediment dynamics (Wang et al., 2011c), delivery of nutrients and pollutants (Zhang et al., 2013; Liu et al., 2012; Bi et al., 2014b).

3.2. Altered hydrological process by the WSRS

During the 1950s when the Yellow River was less fragmented by dams, daily river flow and sediment flux recorded at station Lijin presented a natural rhythm of seasonal signals (Fig. 6A). High water discharge (~3000 m^3/s to 5000 m^3/s) was found in the flooding season from July to September, corresponding to the high precipitation in the middle reaches and the resultant high sediment yield from the loess region. As a result, SSC at station Lijin illustrated a similar pattern in seasonality to the water discharge, as the sediment transport rate in the flooding season was up to several thousands of tonnes per second (Fig. 6A). High suspended sediment concentration of the river water (> 35 kg/m^3) favors hyperpycnal flows at the river mouth that play a primary role in sediment export off the river mouth (e.g., Wang et al., 2010b). In the dry season the river flow was one order of magnitude lower than that in the flooding season except for the drastic decrease induced by the operation of the Sanmenxia Reservoir in 1960. Due to the weak intensity of rainfall in the middle reaches in the dry season, the sediment yield from the loess region decreased significantly, which resulted in a drop of the sediment flux by two to three orders of magnitude in the dry season (Fig. 6A).

Since 2002 the water and sediment discharges to the sea have been primarily regulated by the Xiaolangdi Reservoir as indicated by the impulsive signals instead of the previous natural seasonal rhythm (Fig. 6). Although the peaks of river flow (~4000 m^3/s) were comparable with those in the 1950s, the durations of high water discharge were greatly shortened to be less than one month (Fig. 6B). Based on the daily records at station Lijin (2002–2013) 15 events of WSRS were identified (see also in Table 1) that were characterized by the episodic increases in water discharge and SSC. The maximum river flow, maximum SSC and duration of WSRS varied slightly from 2002 to 2013 (Table 1), mostly depending upon the volume of water that was stored within the Xiaolangdi Reservoir and the upstream reservoirs prior to WSRS. During the non-WSRS periods, the river flow was artificially maintained to be several hundreds of m^3/s together with SSC < 1 kg/m^3 (Fig. 6B). Consequently, the WSRS contributed ~27.8% and ~53.8% of total annual water discharge and sediment load to the sea in average, respectively, within ~20–25 days (Table 1), which greatly modified the natural hydrological cycle. The plots of cumulative sediment load and water discharge to the sea versus cumulative time indicates that in the 1950s about 80% of sediment was delivered to the sea within 20% of time (more than two months every year), corresponding to the flood season (Figs. 6A and 7). However, 80% of the sediment delivery has been concentrated within 10% of time since 2002, corresponding to the short period of WSRS (nearly one month every year) (Figs. 6B and 7).

Compared with the natural seasonal variations of water and sediment with less human interventions in the 1950s, the peaks of SSC did not temporally match those of river flow during the period of 2002–2013 (Fig. 6), which was evidently ascribed to the different operations of reservoir within the WSRS (see Fig. 4). During the first phase

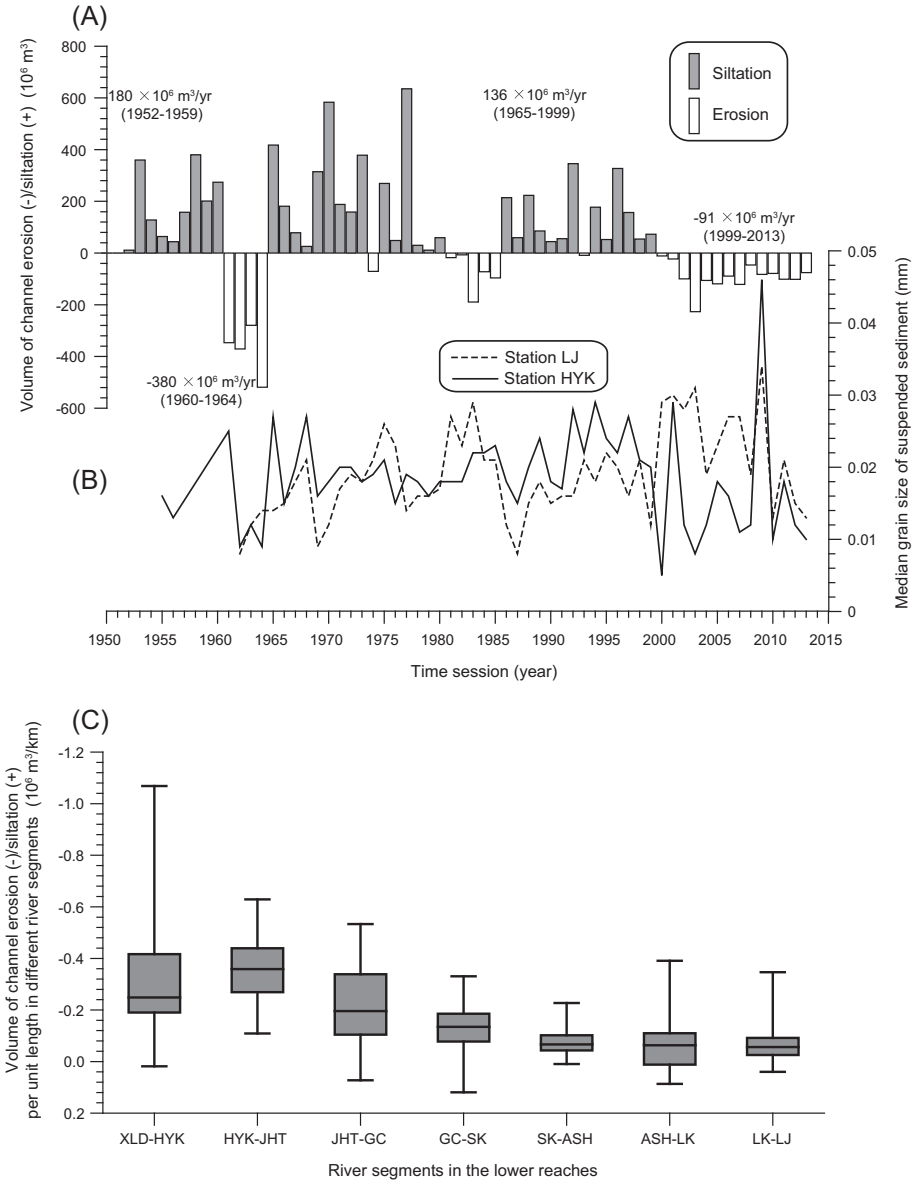

Fig. 9. Volume of channel erosion-siltation in the lower reaches from 1950 to 2013 (A), median grain size of suspended sediment at stations Huayuankou and Lijin (B), and volume of channel erosion-siltation for different river segments downstream the Xiaolangdi Reservoir from 2002 to 2013 (C).

of WSRS the flooding water was released from the Xiaolangdi Reservoir to scour the downstream riverbed; however, this erosional process was not capable of producing high SSC (e.g., Fig. 5A). Peaks of SSC at station Lijin were usually found during the second phase as the Xiaolangdi Reservoir exported the high-concentrated and fine-grained sediment together with a decreasing river flow (Figs. 4B and 5A). The box-whisker plots of daily SSC versus the classified daily river flow indicates that the SSC at station Lijin in the 1950s increased corresponding to the increasing river flow because of enhanced surface erosion in the loess region due to heavy rainfall in the flooding seasons (Fig. 8A). As a result, the maximum SSC usually increased to > 100 kg/m^3 as the river flow exceeded 3000 m^3/s, which yields a rating curve between the SSC and river flow with a coefficient of determination R^2 = 0.79 (Fig. 8A). Dam-regulation since 2002 induced a pattern of high SSC corresponding to moderate river flow (from 2000 to 3000 m^3/s) rather than high river flow (Fig. 8B). As the river flow exceeded 3000 m^3/s the SSC decreased, indicating that the rating curve was no longer applicable. The parabolic-type curve of SSC with river flow suggested the impacts from temporal mismatch between water release and sediment export during WSRS (Figs. 4 and 5).

Peaks of high water discharge and SSC presently appear in late June and early July due to the dam regulation, one or two months before the natural flooding season (July to September, see Wang et al., 2006a). Modification of the river hydrological process might have potential impacts on the aquatic ecosystem in the coastal sea (e.g., biomass, assemblage and biodiversity) since fish, crab, shrimp and planktons would have to adapt to this new hydrological regime.

3.3. WSRS-induced riverbed erosion downstream the Xiaolangdi Reservoir

The siltation in the lower Yellow River has been a major concern for river management as it modifies the channel geometry and impacts the discharge capacity for flooding water. The highly elevated riverbed (see Fig. 2) potentially puts millions of habitants in the low-lying fluvial plain at high risk. Prior to the operation of Xiaolangdi Reservoir in 1999, the lower river bed was mostly silted except for temporary erosion induced by the early operation of the Sanmenxia Reservoir around 1960 and slight erosion in the mid-1980s, even though the annual siltation varied largely year by year primarily depending upon the supply of water and sediment derived from the upper and middle reaches (Fig. 9A). The annual siltation in the lower reaches was estimated at ~101 × 10^6 m^3/yr from 1952 to 1999, equivalent to ~131 Mt/yr of

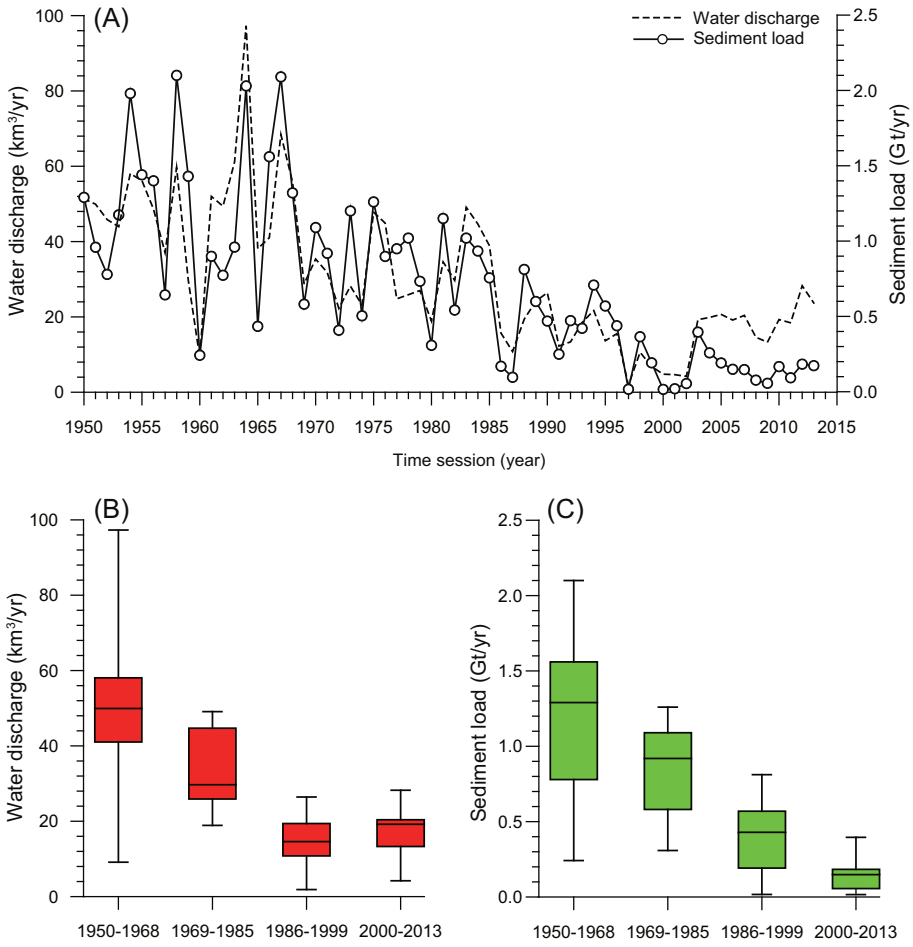

Fig. 10. Annual water discharge and sediment load recorded at station Lijin from 1950 to 2013 (A); Stepwise decreases in water discharge (B) and sediment load (C) to the sea, illustrating the stepwise decrease in water and sediment and the departure of water from the sediment since 2002 as impacted by the WSRS.

sediment deficit to the coastal ocean as the bulk density of sediment is taken as 1.3×10^3 kg/m^3 (e.g., Saito et al., 2001). Since the operation of the Xiaolangdi Reservoir, erosion has become a dominant feature in the lower reaches with an average annual erosion of ~91 $\times$ 10^6 m^3/yr (Fig. 9A), particularly since 2002. Therefore, the channel erosion induced by WSRS contributed ~100 Mt/yr of extra sediment to the sea that was composed of coarser fractions (see Fig. 5).

Grain size of suspended sediments at station Huayuankou and Lijin presented a quick response to the erosion or siltation in the lower channel (Fig. 9B). Siltation in the lower channel was primarily contributed by the settling and accumulation of coarser fraction of sediment (D > 0.025 mm) that bypassed station Huayuankou (Wang et al., 2007). As a result, the suspended sediment at station Lijin is finer than that at station Huayuankou corresponding to the siltation of the lower channel. Erosion in the lower channel supplied a considerable amount of coarser sediment to the sea, as indicated by the suspended sediment at station Lijin being much coarser than that at station Huayuankou, particularly after the construction of Xiaolangdi Dam in 1999 (Fig. 9B). Because of the difference in dam operations between the first and second phases during WSRS (Fig. 4), the increase in sediment grain size at station Lijin primarily resulted from the erosion of the lower riverbed during the first phase, while the fine-grained sediment export from the Xiaolangdi Reservoir during the second phase was directly delivered to the sea and thus had little contribution to the channel siltation (Fig. 5).

Since the WSRS in 2002, all of the river segments downstream the Xiaolangdi Reservoir experienced significant erosion, as the erosive intensity decreased downstream gradually (Fig. 9C). The river segments near the Xiaolangdi Reservoir (e.g., XLD–HYK and HYK–JHT) were highly eroded with annual erosion of 36 $\times$ 10^6 m^3/yr, accounting for ~54% of the total erosion of the lower channel, whereas the erosion in river segments (ASH–LK, LK–LJ) upstream Lijin were only 9–14 $\times$ 10^6 m^3/yr. Nevertheless, channel erosion or siltation is highly dynamic, which significantly modifies the sediment texture of the riverbed, channel geometry and hydraulic slope; these conditions feedback so as to impact the river dynamics and the erodibility of the riverbed.

3.4. Interannual variations of water discharge and sediment load to the sea

Wang et al. (2007) reported the stepwise decreases in both water discharge and sediment load from the Yellow River to the sea during the period of 1950–2005 as dominated by dam regulation and soil conservation practices in the river basin. Prior to the operation of Liujiaxia Reservoir (see Fig. 1) in 1968, the average water discharge and sediment load to the sea were 50 km^3/yr and 1.2 Gt/yr, respectively; nevertheless, high interannual variability was due to less regulation of dams except for the transitory impacts from the Sanmenxia Reservoir (Fig. 10A). The joint operations of Liujiaxia Reservoir (1968) in the upper reaches and the soil-conservation practices in the middle reaches since the mid-1970s subsequently caused stepwise decrease in water and sediment. As a result, the water and sediment at station Lijin decreased by 35% and 30%, respectively, during the period of 1969–1985 (Fig. 10). Furthermore, the combined impacts from the Liujiaxia Reservoir, Longyangxia Reservoir (1985) and the soil-conservation practices continuously reduced the water and sediment to ~15 km^3/yr and 0.4 Gt/yr, respectively, accounting for ~30% of those in the 1950s. The stepwise decreases in both water discharge and sediment load are similar to each other; however, the Xiaolangdi Reservoir that controls the water and sediment derived from the upper and middle reaches (Figs. 1B and 2A) presented different impacts on the water and sediment, as indicated by the evident departure of sediment from the water

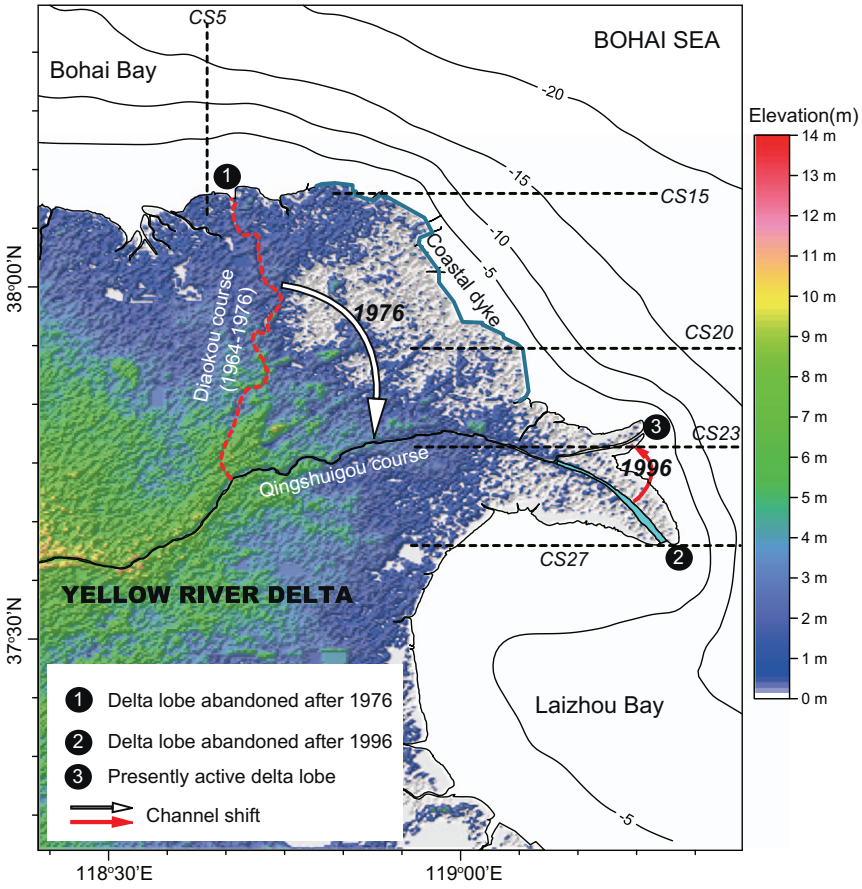

Fig. 11. Relief map of the modern Yellow River Delta showing the abandoned delta lobes and the presently active delta lobe, resulting from the channel shifts in 1976 and 1996. The solid lines indicate the water depth of the subaqueous Yellow River Delta with a contour interval of 5 m. The dashed lines indicated the offshore transects for bathymetric surveys (see Fig. 12).

discharge from 2000 to 2013, particularly after the WSRS (Fig. 9B and C). The recent water discharge to the sea is comparable to that of 1986–1999, whereas the sediment load decreased to 0.14 Gt/yr, approximately 12% of that in the 1950s, which implied that annually averaged SSC decreased drastically.

WSRS has induced changes in sediment source and flux, grain-size of sediment particles and hydrological process (see Figs. 6–10) in the lower reaches. These eventually impacted the process of estuarine sediment dynamics and morphological evolution of the present delta lobe. In-situ observations and numerical modeling confirmed that the dispersal pattern of river-laden sediment and regime of sedimentation at the river mouth have been largely altered by the human interventions in the river basin (Wang et al., 2010b; Wang et al., 2011c).

3.5. Morphological response of the Yellow River Delta to the WSRS

Due to abundant sediment supply over thousands of years, the Yellow River has formed a broad fan delta since the Holocene that mostly consists of silt and fine sand (Saito et al., 2001). It was estimated that approximately 0.5 Gt/yr of sediments were deposited in the alluvial fan. Owing to frequent channel avulsions over the past thousands of years, nine delta superlobes have been formed along with the coast of the western Bohai Sea, together with one located on the western coast of the Yellow Sea (Saito et al., 2001; Fig. 1A). The recently formed delta superlobe with an accretion rate of 25 km^2/yr (Saito et al., 2000), known as the modern Yellow River Delta, has been formed since 1855 as the river reentered the Bohai Sea from the southern Yellow Sea with a subaerial area of > 5000 km^2 (Fig. 1A, Fig. 11). The modern Yellow River Delta has experienced > 50 channel shifts due to rapid channel siltation and resultant channel instability, with major shifts occurring approximately every 10 years (Wu et al., 2015b). The most recent major channel shift happened in 1976 as the river channel on the delta plain artificially migrated southward from the Diaokou course to the Qingshuigou course (Fig. 11), which consequently formed an abandoned delta lobe in the northern part and an active delta lobe in the southeastern part. In 1996, a minor channel shift was artificially implemented as the ending channel shifted northward to form the present delta lobe (Fig. 11).

In contrast to the continuous delta progradation during the initial 100 years (1855–1950s), the Yellow River Delta has experienced a regime shift from a constructive phase to a destructive phase over the past 60 years, as primarily impacted by the stepwise decrease in sediment load from the river to the sea (Fig. 10). The delta lobes that were abandoned after 1976 and 1996 presently suffer significant coastal erosion (e.g., Chu et al., 2006; Wang et al., 2006b; Bi et al., 2014a), whereas the presently active delta lobe since 1996 has prograded seaward due to the accumulation of river sediment. We selected five cross-shore transects that are located on the abandoned delta lobes and on the presently active delta lobe (Fig. 11), respectively, to show the spatio-temporal changes of the subaqueous slope along the Yellow River Delta based on the bathymetric observations. Bathymetric data at transects of CS5 and CS15 (right located at the abandoned Diaokou delta lobe) indicate that the abandoned subaqueous delta slope has experienced strong erosion since 1976 mostly in the upper slope shallower than 10–15 m (Fig. 12A and B), whereas the lower slope was found to be stable or slightly accumulated. The subaqueous slope was eventually reshaped into a gentle form instead of the previous steep one. Wang et al. (2006b) suggested that strong interaction between nearshore wave dynamics and the protuberant topography particularly in wintertime might be the mechanism to the reshaping process of the subaqueous slope. Transect CS20, located between the presently active delta lobe and the abandoned Diaokou delta lobe, experienced a gradual seaward progradation from 1976 to 1988; however, erosion has become a dominant pattern during the recent decades (Fig. 12C),

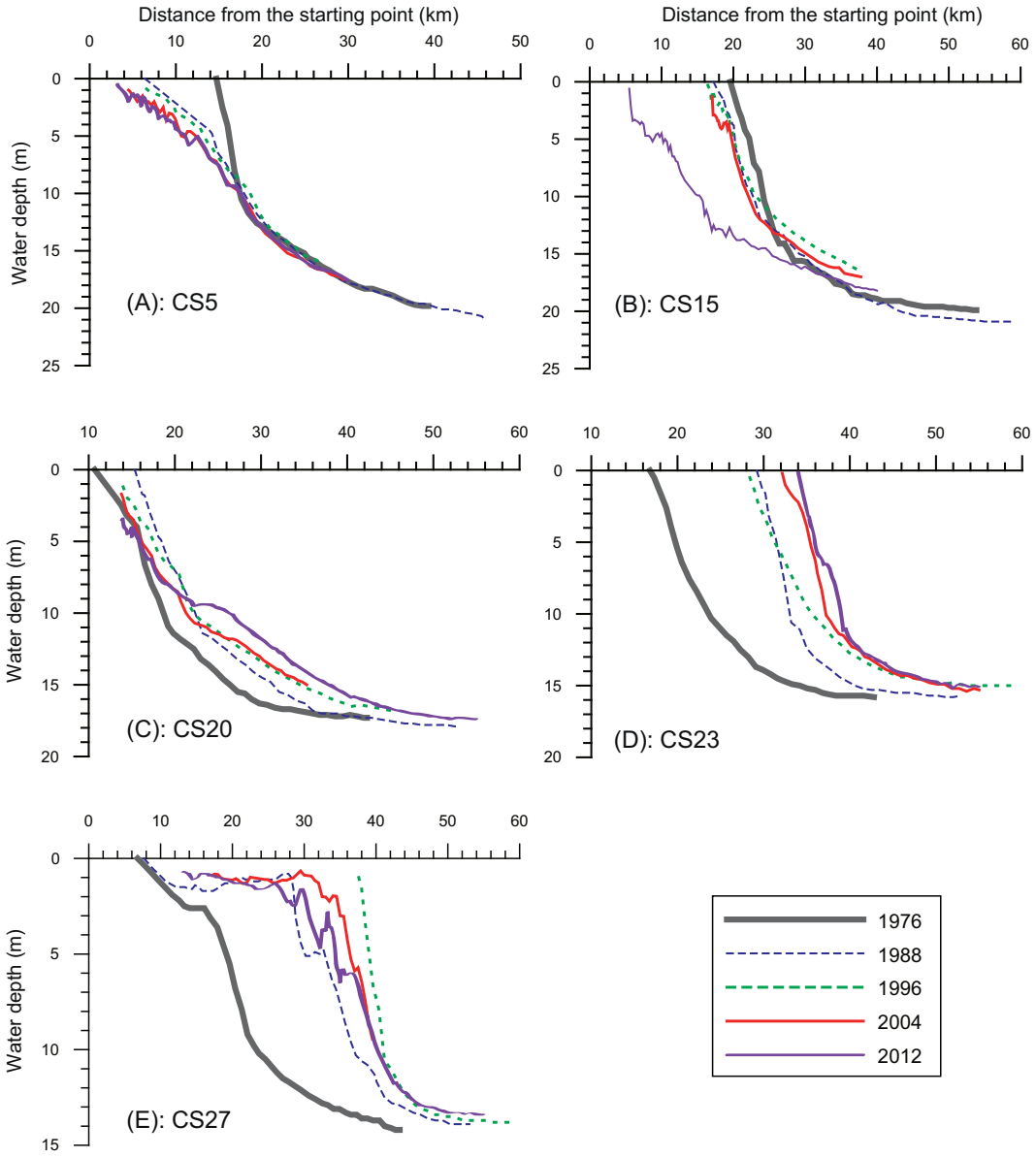

Fig. 12. Bathymetric changes of the subaqueous slope from 1976 to 2012 at the five cross-shore transects along the Yellow River Delta, to show the boundary of the deposition of river-laden sediment.

corresponding to the drastic decrease in river sediment load to the sea (Fig. 10). From 2004 to 2012, slight deposition was found in the lower slope deeper than 10 m, with an accumulation rate of approximately 23 cm/yr, which perhaps indicates the far-field accumulation of river-delivered sediment during WSRS. In contrast, the data at the presently active river mouth (CS23) presented a rapid deposition from 1976 to 1988, in the area shallower than 15 m, with a shoreline progradation rate of 0.8 km/yr and an accumulation rate of ~50–80 cm/yr, respectively (Fig. 12 D). From 1988 to 1996 deposition was found only on the lower slope deeper than 7 m with an accumulation rate of 30–40 cm/yr, whereas the upper slope almost remained unchanged. Wang et al. (2010a) proposed that estuarine hyperpycnal flows induced by high concentration (~30 kg/m^3 in average) of fine-grained sediment (~0.018 mm) favored down-slope transport of sediment and considerable deposition on the lower slope. In contrast, the recent coarsening of suspended sediment (~0.023 mm in median grain size) due to WSRS resulted in deposition mostly on the upper prodelta slope shallower than 12 m (Fig. 12D), with an accumulation rate of 18–46 cm/yr, even though the annual sediment load was decreased drastically to be only 0.15 Gt/yr (Fig. 10). The coarser sediment derived from channel erosion during the first phase of WSRS seemed to be directly contributing to accretion of the present river mouth, as several river mouth bars were formed during the early period of WSRS, which made the pathway of the river plume highly unstable (e.g., Wang et al., 2005). Bathymetric changes on transect CS27 (right off the 1996 abandoned delta lobe, see Fig. 11) illustrate a rapid deposition at the river mouth that was previously active from 1976 to 1996, as well as a notable shoreline progradation rate of ~1.6 km/yr (Fig. 12E). Since the channel shift in 1996, continuous erosion in the upper slope (< 10 m in water depth) has been dominant due to the combined impacts of cutting off the sediment supply and the highly energetic receiving basin environment. The successive erosion from 1996 to 2012 implies that the river-delivered sediment has had little contribution to the sedimentation of the abandoned delta lobe (Fig. 12E).

In summary, coastal erosion has been a dominant feature of the Yellow River Delta except for the local deposition around the presently active river mouth that receives most of the river sediment delivered to the sea during the WSRS (Fig. 11). The WSRS-induced coarsening of

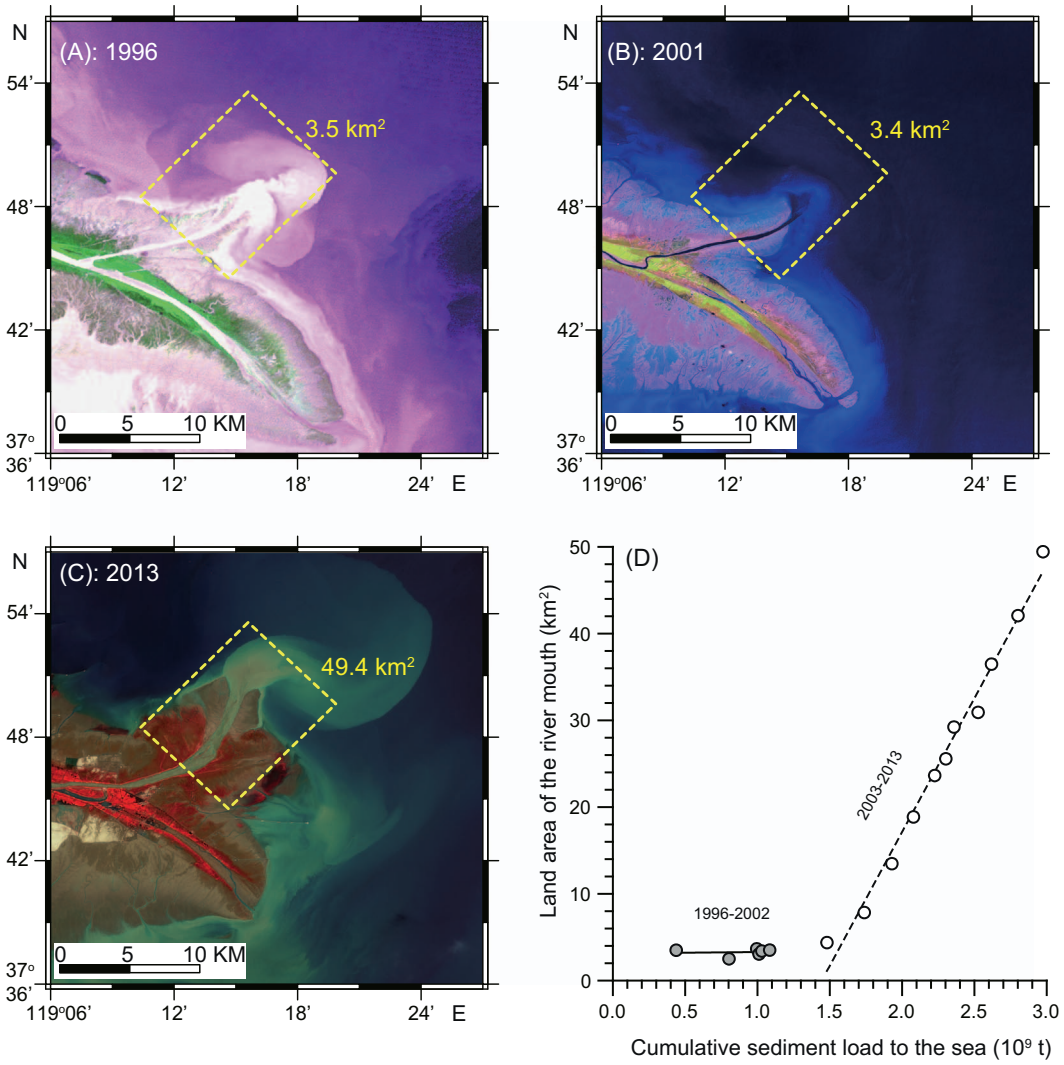

Fig. 13. LANDSAT imageries of the Yellow River Mouth in 1996 (A), 2001 (B) and 2013 (C); and scatter plot of cumulative sediment load versus the accretion of land area of the presently active delta lobe from 1996 to 2013 (D). The square with dashed line shows the domain for calculating the land area of river mouth. And the numbers indicate the land area (km^2) of delta lobe within the square.

suspended sediment delivered to the sea was expected to play a critical role in the sedimentation of the present river mouth (Wu et al., 2017). We selected a small region (~115 km^2 in area) that covers the present river mouth to investigate the changes of land area from 1996 to 2013 (Fig. 13). Coastlines were extracted from LANDSAT imagery based on a combination of histogram threshold and band ratio techniques (Alesheikh et al., 2007; Bi et al., 2014a). The datasets indicate that there was almost no significant change in land areas from 1996 to 2002 (Fig. 13A and B), when the corresponding sediment load to the sea was ~0.16 Gt/yr. However, the land area increased dramatically from 2003 to 2013 with an annual accretion rate of ~4.5 km^2/yr (Fig. 13C and D), even though the sediment load to the sea (~0.17 Gt/yr) was almost the same as that of 1996–2002. Such a surprising change in accretion rate of present river mouth suggests the dominance of increasing grain size of suspended sediment during the first phase of WSRS (Fig. 5B). These coarser sediments derived from the lower channel are expected to deposit locally at the present river mouth, which consequently contributes much to the delta accumulation in the area shallower than 10 m (Fig. 12D).

The dispersal and accumulation of river-delivered sediment during the WSRS were confirmed by the changes in composition of surface sediment off the present river mouth. Three cruises were conducted before (in May), during (in July) and after (in September) the WSRS in 2010 in order the sample the surface sediments around the present river mouth (Fig. 14A). Between the field surveys from May to September, prevailing southerly winds at the river mouth produced an average significant wave height of ~0.5 m (Wang et al., 2014b). Before the WSRS the nearshore surface sediment at the river mouth was mostly dominated by sand and silt with percentages of 57% and 38%, respectively, the median grain size of which was approximately 0.07 mm (Fig. 14B), which represents the composition of surface sediment after modification by strong dynamics in the winter-spring seasons. During the first phase of WSRS the suspended sediments sampled at station Lijin were mostly dominated by silt and sand with percentages of 72% and 22%, respectively, as a result of channel erosion in the lower reaches (Figs. 4 and 5). Consequently, the silt content in the nearshore surface sediment increased after the first phase of WSRS, while the clay content kept unchanged (Fig. 14B). The input of fine-grained sediment during the second phase (Figs. 4 and 5) made the nearshore surface sediment finer as the clay content increased to 15–30%, whereas the silt was still a dominant component with a percentage of 62–69% (Fig. 14B). However, the contents of silt and clay in the suspended sediment at station Lijin during the second phase accounted for ~69% and 24% of the total sediment, which implies more fine-grained sediment was transported offshore during this period. In contrast, the offshore surface sediment was mostly dominated by silt (contents ranging

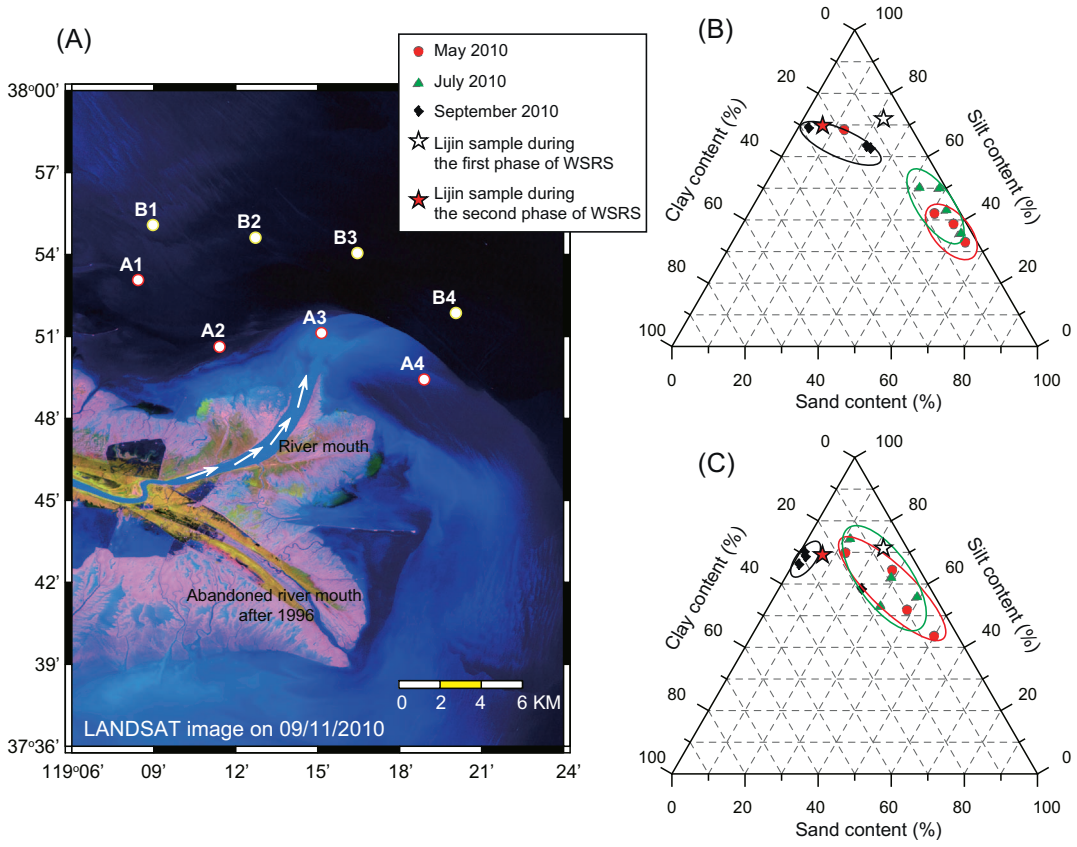

Fig. 14. Changes of surface sediment composition off the presently active delta lobe before, during and after the WSRS in 2010: (A) sampling stations; (B) changes in composition of surface sediments sampled at stations near the river mouth (A1, A2, A3 and A4); (C) changes in composition of surface sediments sampled at stations far from the river mouth (B1, B2, B3 and B4).

from 44% to 74%) rather than sand before WSRS, with median grain size (~0.03 mm) much less than that of nearshore surface sediment. However, no significant change was found after the first phase of WSRS (Fig. 14C), perhaps because the coarser sediment derived was primarily deposited in the nearshore area. The September cruise found that the offshore surface sediment became much finer with a median grain size of 0.007 mm, approximately one order of magnitude lower than that before the second phase of WSRS. Although the silt was still a dominant component (58–70%), the clay content increased significantly to ~30%, which presented a highly similar composition to that of suspended sediment at station Lijin (Fig. 14C). The spatio-temporal changes in composition of surface sediment at the river mouth suggested that the coarser sediments derived from the lower channel during the first phase of WSRS were mostly deposited in the nearshore area given their high settling velocity, corresponding to the high accretion rate of land area since 2003 (Fig. 13). However, the fine-grained sediments that were directly derived from the Xiaolangdi Reservoir during the second phase of WSRS were transported offshore and accumulated in the less energetic environment, as indicated by the evident deposition in the lower slope of transect CS20 (Fig. 12C). Therefore, the morphological change of the river mouth was not only impacted by the flux of sediment delivered to the sea, but also more depending upon the grain-size composition of sediment.

3.6. Biogeochemical implications of the WSRS to the coastal environment

Given the dominance of WSRS on the delivery of river water and sediment to the sea, a large amount of nutrients (such as carbon, nitrogen, phosphate and silicate) and pollutants (such as heavy metals and PAHs) were transferred to the coastal ocean during the short period of WSRS, which therefore impacted estuarine and coastal geochemical processes and the ecosystem. Based on long-term sampling and analysis, Zhang et al. (2013) estimated that ~56% of annual POC flux was delivered to the coastal sea during the WSRS, as an indication of human disturbance on the transport of terrestrial organic carbon, although this carbon is substantially pre-aged and mostly derived from paleosol deposits outcropping in the loess region (Wang et al., 2012; Tao et al., 2015). Data of daily POC flux (Zhang et al., 2013), in combination with those of daily river discharge, SSC and median grain size of suspended sediment at station Lijin during the WSRS in 2008, illustrated different responses of POC transport to the dam regulations during different phases of WSRS (Fig. 15A). The POC concentration was very low (~4.1 mg/L) before the WSRS, but it increased considerably to be 13.8 mg/L during the first phase of WSRS, as the sediment particles derived from the lower channel erosion were relatively coarse with low capability of absorption (Fig. 15A). During the second phase of WSRS, the POC concentration increased exponentially to be > 100 mg/L, corresponding to the fine-grained sediment exported from the Xiaolangdi Reservoir (Fig. 4). The Xiaolangdi Reservoir acted as a sink for POC that mainly originated from the loess region (Zhang et al., 2013), but transited to be a major source of POC to the sea during the second phase of WSRS. In addition, the concentration of total particulate phosphorus presented a similar pattern to that of POC during the WSRS in 2008 (Fig. 15B). The WSRS evidently increased the particulate phosphorus concentration to be one or two orders of magnitude higher than before the event. As a result, ~78% of the annual flux of particulate phosphorus was delivered to the sea during WSRS, in particular during the second phase when the fine-grained sediment was exported from the reservoir (Wei et al., 2011).

The WSRS in 2009 did not produce high sediment delivery to the sea as expected, although the water discharge was comparable to that in 2008 (Table 1). Approximately 37 Mt of sediment was contributed

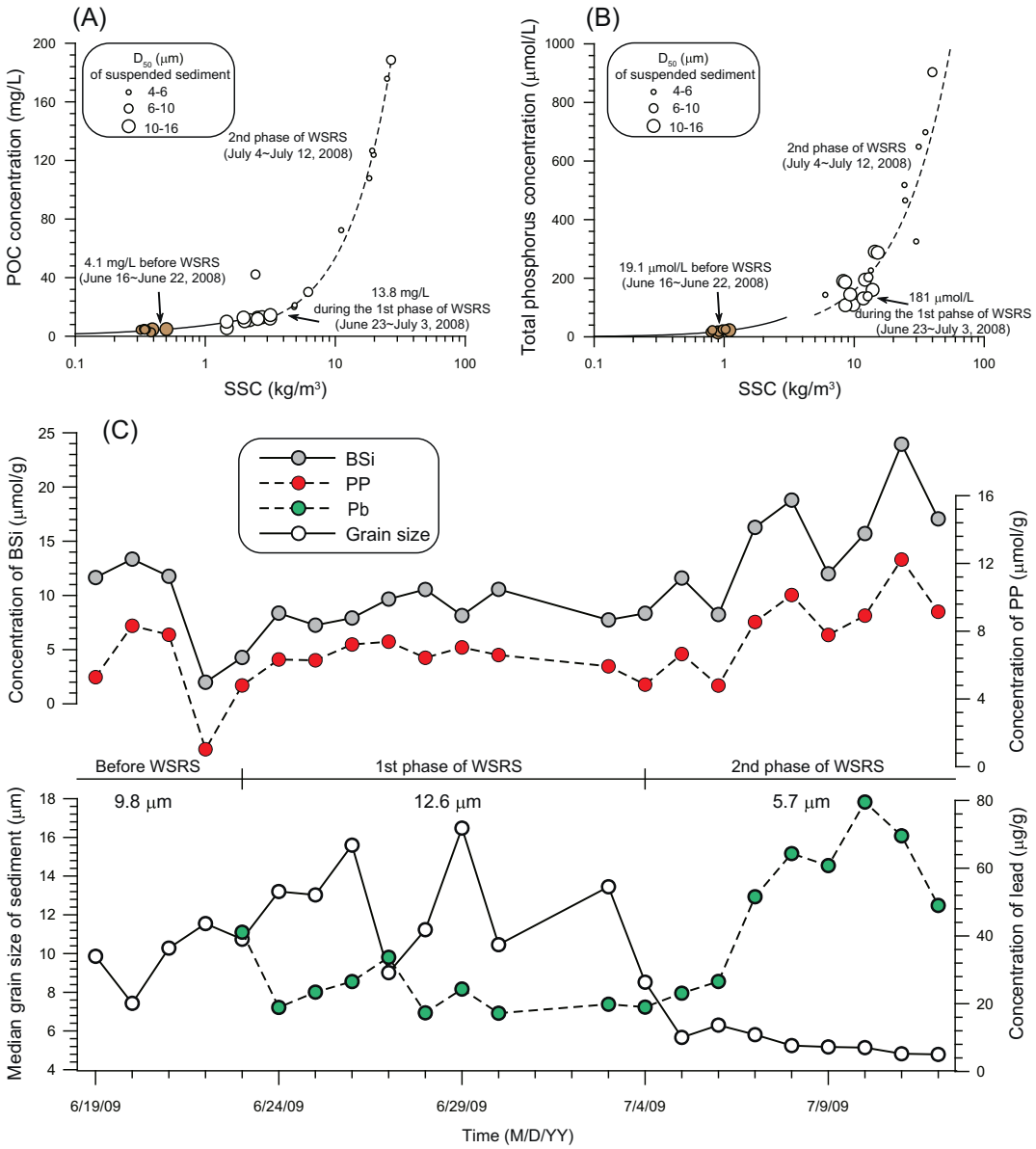

Fig. 15. Dominance of grain size of sediment and SSC during WSRS on the delivery of nutrients and pollutants: (A) particulate organic carbon (POC) concentration versus suspended sediment concentration (SSC) during WSRS in 2008; (B) concentration of total particulate phosphorus (TP) versus SSC during WSRS in 2008; and (C) daily variations of biogenic silica (BSi), particulate phosphorus (PP), lead (Pb) during WSRS in 2009. The circles in Panels (A) and (B) with various sizes indicate the different classification of median grain size (D_{50}) of suspended sediment.

during the first phase due to channel erosion, whereas only 3.6 Mt of fine-grained sediment was exported from the Xiaolangdi Reservoir, as indicated by the low SSC during the WSRS in 2009 (Fig. 6B). Despite the exceptionally low SSC (~8.7 kg/m^3) in 2009, the WSRS still played a critical role in delivering the dissolved and particulate nutrients to the sea, as indicated by both the nutrient concentrations and their fluxes (Liu et al., 2012; Liu, 2015). In particular, the concentrations of biogenic silica (BSi) and particulate phosphorus (PP) that are absorbed by fine-grained sediment particles presented clear responses to the varying grain size of suspended sediment (Fig. 15C). During the second phase of WSRS when the median grain size of suspended sediment decreased drastically to be 4–8 μm, the concentrations of BSi and PP increased to be two times greater than during the first phase, even though the SSC was only one third of that during the first phase. Due to the high water discharge during the WSRS, the daily fluxes of BSi and PP were ~100 times of that prior to WSRS, which presented critical impacts on the coastal primary production and species composition due to the phosphorus limitation for phytoplankton growth in the coastal area (Liu et al., 2012). Given the dominance of grain size of suspended sediment particles over the delivery of particulate nutrients, we speculate that there might be considerable under-estimations of nutrient fluxes from the river to the sea if the samples were taken only during the non-WSRS period (e.g., Pan et al., 2013).

Besides the notable contributions to nutrient delivery, the WSRS also induced high discharge of particulate heavy metals (PHMs) that were bounded to fine-grained sediment (e.g., Bai et al., 2012). Bi et al. (2014b) estimated that > 57% of the annual flux of PHMs from the Yellow River to the sea was transported during WSRS, primarily within the second phase when the Xiaolangdi Reservoir exported the fine-grained sediment that has high capacity of absorption. For example, the lead (Pb) concentration during the second phase of WSRS in 2009 seemed to be 2–3 times higher than that observed in the first phase, associated with the transport of fine-grained sediment (Fig. 15C), even though the SSC was only 3.4 kg/m^3. The WSRS-delivered PHMs and PAHs (e.g., Dong et al., 2015) would be transported into the coastal sea and eventually accumulated in the coastal region, which induced

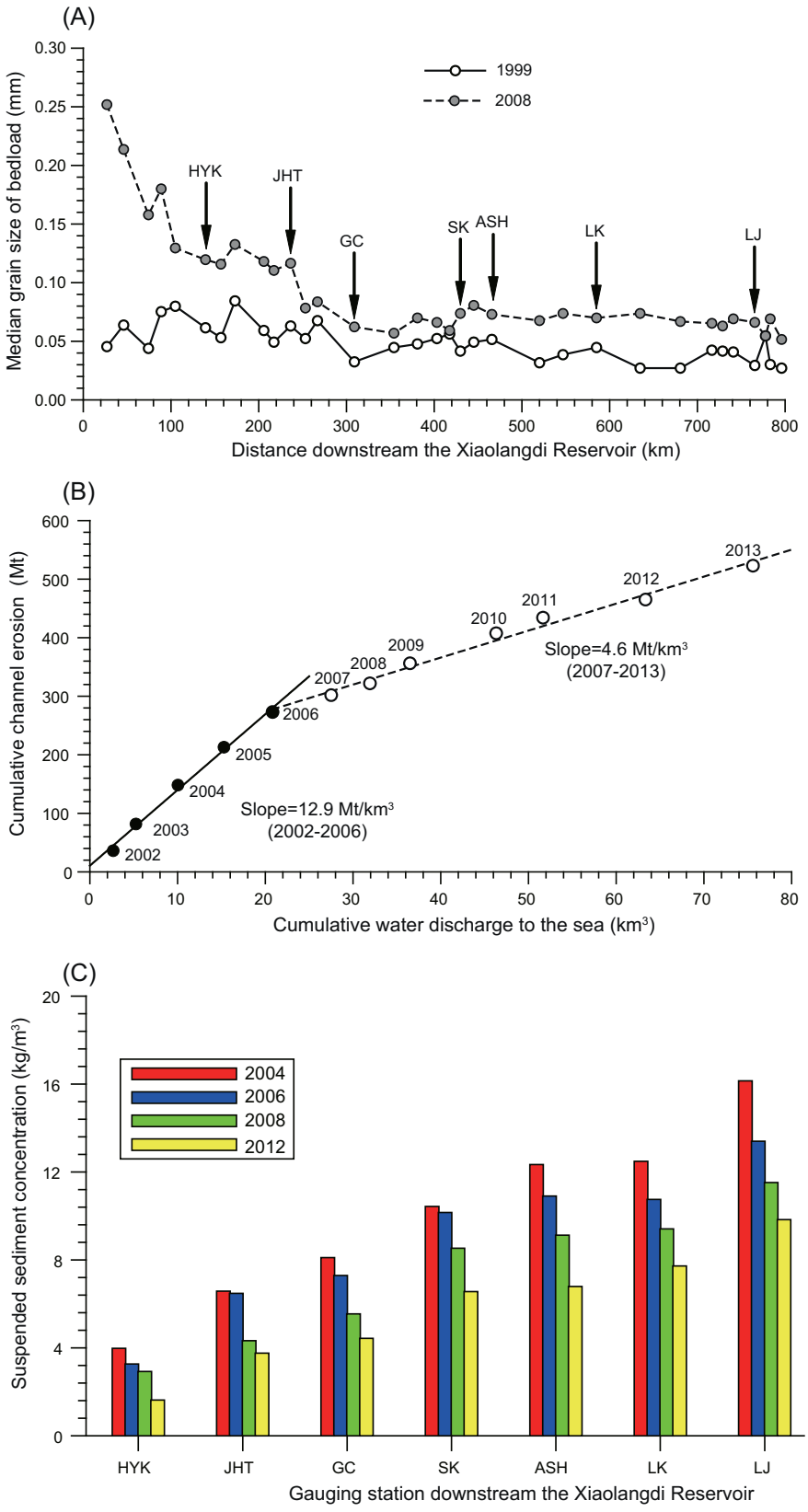

Fig. 16. Change in median grain size of bed load in the lower reaches downstream the Xiaolangdi Reservoir (A); and the plot of cumulative water discharge to the sea versus the lower channel erosion during the WSRS from 2002 to 2013 (B), illustrating the deceasing contribution of lower channel erosion to the sediment flux to the sea since 2006 because of sediment coarsening on the lower riverbed; and the SSCs at downstream gauging stations during the first phase of WSRS (C).

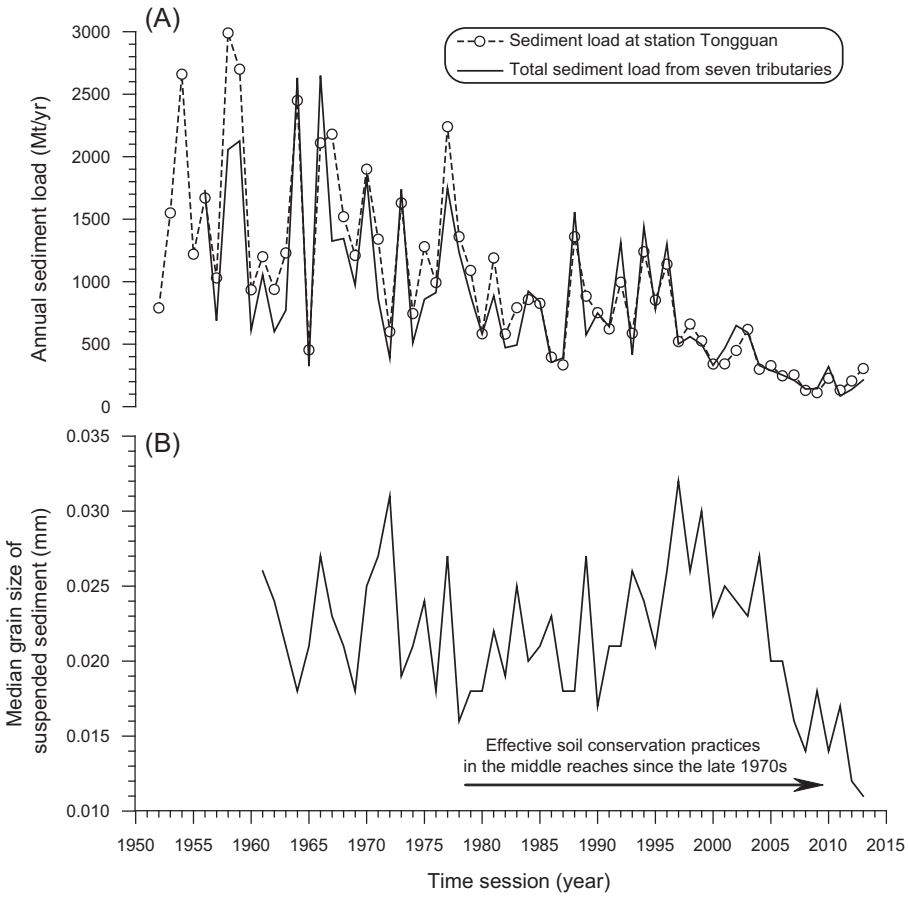

Fig. 17. Time-series data (1950s–2013) of sediment yield from seven major tributaries (locations shown in Fig. 1) in the loess region and sediment load at station Tongguan (A), and the annual median grain size of suspended sediment at station Tongguan (B), presenting significant impact of soil-conservation practices on sediment delivery to the mainstream of the Yellow River.

evident pollution in the soils of coastal wetlands (Bai et al., 2012) and is expected to potentially trigger environmental risks.

4. A perspective on the WSRS of the Yellow River

4.1. How much sediment could be delivered to the sea by WSRS in the future?

The sources of sediment delivered from the Yellow River to the sea during the WSRS include: 1) the channel erosion downstream the Xiaolangdi Reservoir during the first phase that mostly derived coarser sediment; and 2) the sediment directly exported from the Xiaolangdi Reservoir during the second phase with a median grain size of < 0.01 mm (Figs. 4 and 5). Together with the implementation of WSRS year by year, the composition of sediment on the lower riverbed has changed much due to significant channel erosion over the past 10 years. In 1999, when the Xiaolangdi Reservoir was completed, the median grain size of sediment on the riverbed downstream the reservoir was < 0.09 mm with a slightly downstream fining trend (Fig. 16A). The coarser fraction (D > 0.025 mm) of sediment bypassing station Huayuankou mostly deposited in the lower reaches. As a result, the sediment on the lower riverbed was much coarser than the suspended sediments at stations Huayuankou and Lijin except for the period of channel erosion (Fig. 9A and B). However, the sediment on the lower riverbed has become much coarser ten years after the completion of Xiaolangdi Reservoir, as the median grain size of bed sediment increased by 2–5 times in the downstream river segments (e.g., XLD-HYK and HYK-JHT) near the Xiaolangdi Reservoir where channel erosion was highest (Figs. 9B and 16A). These changes imply that the lower riverbed has become armored by the coarser sediments due to channel erosion and it would become more and more difficult to erode these sediments given the artificially controlled maximum water flow of 4000 m^3/s during WSRS. The plot of cumulative channel erosion versus the cumulative water discharge during WSRS from 2002 to 2011 illustrated an evident change from 2007 (Fig. 16B). The slope of linear regression in the period of 2007–2013 was much lower than that of 2002–2006, indicating the sediment derived from lower channel erosion has significantly decreased. The SSCs at downstream stations during the first phase of WSRS presented a generally downstream increase because of overall erosion of the lower riverbed by the clear water released from the Xiaolangdi Reservoir (Fig. 4); however, the SSCs at all downstream stations decreased year by year (Fig. 16C), corresponding to the gradually decreasing channel erosion (Fig. 16B). Unless the river flow increases significantly in the future, the sediment derived from the channel erosion would decrease year-to-year.

The sediment export from the Xiaolangdi Reservoir was mostly dominated by the volume of water released from the reservoirs (e.g., the Wanjiazhai and Sanmenxia, see Fig. 1) upstream the Xiaolangdi Reservoir and the volume of sediment accumulated within the Xiaolangdi Reservoir. There are large uncertainties in water discharge upstream the Xiaolangdi Reservoir, since the precipitation in the middle reaches seems to be closely associated with the signal of climatic oscillation such as the ENSO events (Wang et al., 2006a, 2011a). In addition, the increasing water demands from the millions of people in the upper and middle reaches enhance the water consumption for domestic use and agricultural irrigation (Wang et al., 2006a).

The sediment yield from the loess region has also experienced drastic decrease since the past 60 years, particularly since the mid-1980s (Fig. 17A). Station Tongguan, right upstream the Sanmenxia Reservoir (see Fig.1), recorded sediment derived from both the upper reaches and the loess region. The annual sediment load at station Tongguan illustrates a decreasing trend similar to the total annual sediment load derived from the seven major tributaries in the loess region (see Fig. 1), as the sediment load over the recent 10 years was

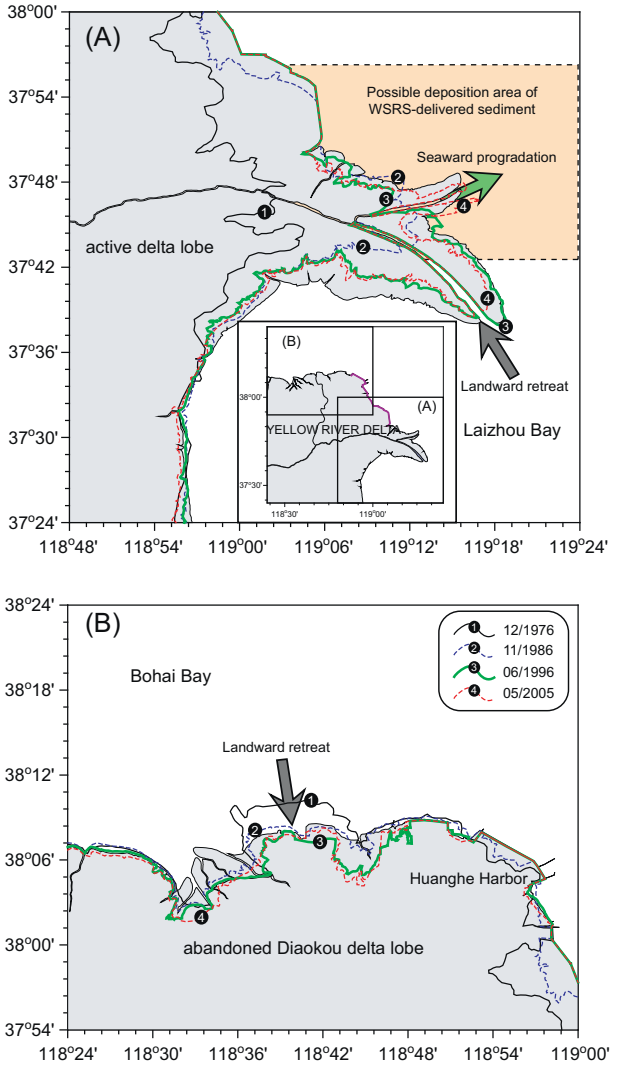

Fig. 18. Changes of the coastline along the Yellow River Delta from 1976 to 2005: (A) the active Qingshuigou delta lobe, and (B) the abandoned Diaokou delta lobe. The coastlines were extracted as the low-tide lines from the LANDSAT imageries. The dashed line in Panel (A) indicates the possible domain for the accumulation of river sediment discharged during WSRS. (For interpretation of the references to colour in this figure legend, the reader is referred to the web version of this article.)

~260 Mt/yr, accounting for ~14% of that in 1950s (Fig. 17A). This decrease is mostly ascribed to the soil-conservation practices in the middle reaches since the 1970s as the land cover has been effectively improved (Wang et al., 2007). Correspondingly, the median grain size of suspended sediment at station Tongguan has drastically decreased over the past ten years (Fig. 17B). Therefore, the significant decrease in sediment entering the Xiaolangdi Reservoir implies that the siltation within the reservoir will decrease and the depocenter of fine-grained sediment will move towards the dam. In fact the continuous decrease of reservoir storage capacity indicates significant sediment retention within the reservoir in despite of the efforts of WSRS (Fig. 3B), as confirmed by the fact that the annual sediment load exported from the Xiaolangdi Reservoir only accounts for ~25% of that at Sanmenxia (right upstream the Xiaolangdi Reservoir) since 2002.

Consequently, the WSRS in the future will face an armored lower riverbed, a decreasing sediment supply from the middle reaches and an unpredictable water discharge of the Yellow River. The WSRS-induced sediment supply to the coastal ocean is therefore expected to be decreasing continuously, which will enhance the coastal erosion of the Yellow River Delta.

4.2. Delta evolution under the WSRS in the future

Due to insufficient sediment supply as a result of human intervention in the river basin over the past several decades, the modern Yellow River Delta is in decline in contrast to the rapid progradation over historical times. Besides the enhanced coastal erosion in the subaqueous delta (Fig. 12), the shoreline retreat indicates a rapidly shrinking subaerial delta. The changes of shoreline with 10–year interval, as extracted from the LANDSAT imagery, illustrated that the present Qingshuigou delta lobe experienced a rapid progradation during the period of 1976–1986 as the river channel was artificially shifted to the present course from the Diaokou course in 1976 (Fig. 18A). During this period the unchannelized river flow dumped the river-laden sediments over a large area, which produced rapid progradation of the subaerial delta and accumulation in the subaqueous delta (Figs. 12 and 18A; Wu et al., 2015b). Since the mid-1980s the channelized river flow facilitated by hardened levees favored the rapid southeastward progradation of the river mouth; as a result, evident shoreline progradation (~1.6 km/yr) mostly appeared around the river mouth during the period of 1986–1996 (Figs. 12E and 18A). After the channel shift in 1996 (see Fig. 11), the shoreline of the abandoned river mouth retreated landward together with continuous erosion on the upper subaqueous slope (Figs. 12E and 18A). In contrast, the newly formed river mouth prograded seaward during the period of 1996–2005 as a result of rapid deposition of WSRS-derived coarser sediment right off the river mouth (Figs. 12 and 18A). In the northern part of the delta where the abandoned Diaokou delta lobe is located, the shoreline retreated landward continuously after 1976 due to the cutting-off of river sediment supply and strong coastal dynamics (Wang et al., 2006b), as confirmed by the significant erosion in the upper subaqueous slope (Figs. 12A and B; 18B).

Both the previous progradation and recent decline of the modern Yellow River Delta were impacted by the river sediment supply including the flux, grain-size composition and temporal distribution, as well as the associated sediment dynamics at the river mouth. The WSRS-induced changes in SSC and grain size of sediment particles have altered the sediment transport at the river mouth transiting to buoyant surface plume from the previously dominant hyperpycnal plume, and triggered rapid response of the deltaic erosion-accumulation pattern (e.g., Wang et al., 2010a, 2010b; Wang et al., 2011c). Both the sediments derived from the lower channel erosion and the accumulation within the Xiaolangdi Reservoir were found to be deposited within a limited spatial range around the present river mouth (Fig. 18A), as indicated by the changes in grain-size of surface sediment and bathymetric changes of the subaqueous slope (Figs. 12–14). Given the continuously decreasing sediment supply, the accumulation around the present river mouth would be a local morphological phenomenon, and thus have little contribution to the delta progradation because the sediment accumulation in summertime could not make up the sediment removal by the highly energetic winter storms (Yang et al., 2011b; Wang et al., 2014b). The modern Yellow River Delta will continue to be eroded in the future. If the impacts from sea-level rise and delta subsidence driven by both natural and anthropogenic forcings (e.g., Higgins et al., 2013; Zhang et al., 2015) are taken into account, the delta remains at high risk (e.g. Syvitski et al., 2009). It was estimated that the area of subaerial delta would decrease by 16% as impacted by the coastal erosion and sea-level rise (Ding et al., 2013). Consequently, increasing risks arising from basin-wide human activities, regional water management, delta subsidence, global sea-level rise, and climate extremes will present great challenges to sustaining the regional economic-societal development (Tessler et al., 2015).

4.3. Response of the coastal ecosystem to WSRS in the future

Owing to the rapid delivery of freshwater and sediment to the sea during WSRS, the concentrations of phosphate and dissolved silicate

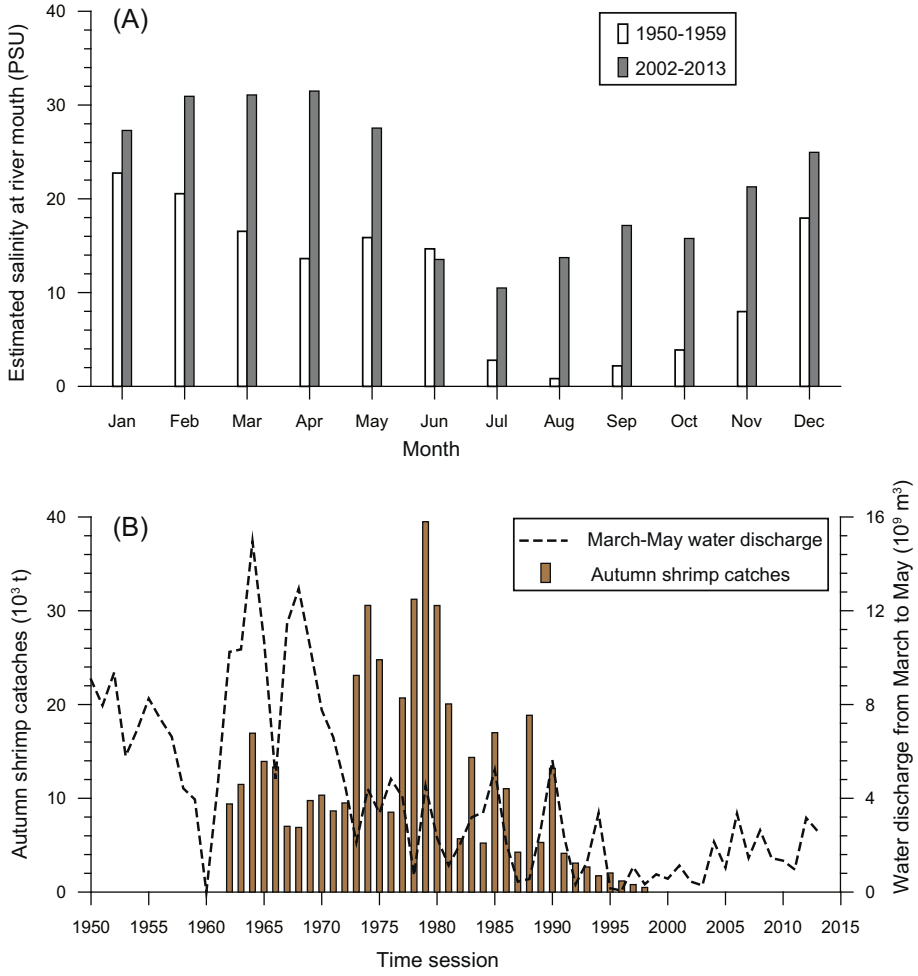

Fig. 19. Estimated monthly salinity at the Yellow River mouth based on the water discharge during the 1950s and the period of 2002–2013 (A); and the comparison between annual catches of Chinese Shrimp and the water discharge from March to May (B).

increased to be three times of the normal level with transport fluxes increasing by 8–30 times due to the high water discharge (Liu et al., 2012). High nutrient loads and nutrient imbalance induced by the WSRS potentially influenced the biomass and community structure of phytoplankton in the coastal sea as the river plume during WSRS extended offshore as far as 24 km away from the present river mouth (Wang et al., 2011b). Future decrease in SSC and the associated decreasing capability of absorption will be unfavorable to the transport of particulate phosphate and therefore increase the flux of dissolved phosphate, and water quality problems (e.g., eutrophication) may irreversibly occur in this large ecosystem (Pan et al., 2013). Nevertheless, the existing limited datasets are still insufficient to understand the impacts of WSRS on coastal nutrient dynamics and the phytoplankton community.

Besides the altered nutrient delivery, the pollutants such as heavy metals and PAHs were rapidly delivered to the sea during the short period of WSRS, which was mostly associated with the transport of fine-grained sediment during the second phase of WSRS (Bi et al., 2014a; Dong et al., 2015). These pollutants were transported and accumulated along with the fine-grained sediment, resulting in heavily contaminated coastal wetlands. Bai et al. (2012) reported the WSRS-induced accumulation of arsenic (As) and cadmium (Cd) in the wetland soils around the river mouth, indicating a degraded quality of coastal wetland and potential threats to the ecosystem.

The Chinese Shrimp (*Penaeus chinensis*) has been one of the traditional economic products in the Bohai Sea, particularly around the Yellow River Mouth where its spawning and nursery grounds are located (Deng and Zhuang, 2001; Jin, 2001). Every year the overwintering population of Chinese Shrimp migrates to the estuaries in the Bohai Sea in March and April to seek the spawning ground where the water temperature is 15–18 °C with salinity ranging from 8.8 to 25.8 PSU (Liu, 1990; Sun and Yang, 2010). From June onwards, the post-larvae begin growing in the nursery grounds with a suitable salinity range of 20–28 PSU (Dong et al., 2002). Therefore, the water salinity associated with river water supply, besides the nutrients, plays a critical role in the life cycle of Chinese Shrimp. A relationship between salinity in estuary and daily freshwater inflow proposed by Sun and Yang (2010) allows us to estimate the salinity change at the river mouth induced by WSRS:

$$S = 37.508e^{-0.001Q} \quad (R^2 = 0.99)$$

where S is the estimated salinity in the estuary in PSU and Q is the daily water discharge (m^3/s).

Compared with the seasonal distribution of potential salinity in the estuary in the 1950s, the WSRS induced significant increases in salinity at the river mouth as the average salinity from March to May, corresponding to the critical period of spawning, was nearly 30 PSU, approximately 2 fold greater than during the 1950s and much higher than the preferred salinity range for spawning of Chinese Shrimp (Fig. 19A). The salinity in June since 2002 was comparable to that of 1950s (13.5 PSU); however, the high water discharge lasted only for ~10 days. The subsequent increase in potential salinity in the estuary was evidently unfavorable to the growth of post-larvae. The artificial regulation resulted in the estuarine salinity increasing by 10 PSU as compared with that in the 1950s, coinciding with the estimation by Lin et al. (2001). In addition, the human-regulated hydrological process does not match the life cycles of coastal inhabitants (e.g., Chinese Shrimp), as the river flow has been artificially delayed by two months

compared with the natural rhythm (Fig. 19A). Consequently, the environment for the spawning and nursery of Chinese Shrimp has been greatly destroyed, particularly due to the WSRS. As a result, the autumn catches of Chinese Shrimp in the Bohai Sea have been declined since 1980, together with decreasing water discharge from March to May when the shrimp migrates from marine environment towards estuarine environment for spawning (Fig. 19B). In the late 1990s, the Chinese Shrimp almost disappeared, which was primarily ascribed to the destruction of spawning and nursery grounds and overfishing during the past 20 years (Jin, 2001). Since 2000 the artificial stock enhancement of Chinese Shrimp in the Bohai Sea has been regionally initiated and resulted in a slight recovery of shrimp catches (e.g., 2300 and 5270 tonnes in 2009 and 2010, respectively) (Li et al., 2012); however, this may not be indicative of recovery for the damaged ecosystem.

When human impacts on the Earth surface were gradual, the ecosystem was considerably resilient; nowadays, high anthropogenic pressures have been transferred to different components within ecosystem in myriad ways. The result is the loss of resilience and adaptability of the ecosystem (Syvitski, 2012). The impacts of WSRS on the coastal ecosystem seem to be considerably profound. The lack of long-term monitoring data makes it difficult to understand the responses of different components of ecosystem to the human interventions in the river basin.

5. Conclusion

Dam-orientated water and sediment regulation in the Yellow River is an unprecedented hydraulic engineering as humans utilize advanced technology to tame a large river with an extremely high sediment load, a symbol of a natural force that has been historically feared and revered over thousands of years. The implementations of WSRS generally achieved its initial hydrological objectives, including the effective erosion of the lower channel bed and increasing the capability of flooding water to mitigate siltation within the reservoirs. Hydrological experiments and observational data are critical to determine the threshold discharges of water and sediment to maintain the erosion-accumulation balance in the lower reaches.

However, significant impacts have been identified on the delta morphology and coastal ecosystem ten years after the WSRS, which was unexpected at the beginning of engineering efforts. The coarser sediment that was derived from channel erosion during the first phase of WSRS has directly contributed to the rapid accretion of the present river mouth, whereas the delta was sediment-starved and declined due to insufficient sediment supply and regime shift of sediment transport process. The fine-grained sediment that was exported from the Xiaolangdi Reservoir during the second phase of WSRS seemed to be a critical carrier of nutrients and pollutants. The human-altered hydrological cycle, enhanced delivery of nutrient and pollutants and the changing estuarine environment presents unpredictable impacts on both terrestrial and aquatic ecosystem in the delta region. These depict a scenario that the signals of human activities in the river basin have been transferred along the hydrological pathway to the coastal system and remotely transformed different components of coastal environment, and thus confirm that humans are modifying the river-coast system in ways that go well beyond climate change. In the future, the sediment yield from the loess region is expected to be decreasing continuously, and the lower channel erosion will be decreased as the riverbed is armored by coarse sediment. These, in combination with the uncertain water discharge that is dominated by climate change and increasing water demands in the river basin, will put the mega-delta and coastal ocean at high environmental risks. Therefore, an integrated management of the river-coast continuum is crucially important for the sustainability of the whole river-delta system. Communication and cooperation between scientists, public and administrators are thus critical to finding a sustainable future for the livelihood in this region. This review on the impacts of river regulation on the river-coast continuum provides an important reference to the management of large rivers worldwide.

Acknowledgement

We appreciate the constructive comments from the reviewers that improved the science and quality of the original manuscript. This work was supported by Ministry of Science and Technology of China (No. 2016YFA0600903), the National Science Foundation of China (NSFC, No. 41376096, 41525021 and 41476069), Aoshan Talents Program supported by Qingdao National Laboratory for Marine Science and Technology (No. 2015ASTP-0S03). Yoshiki Saito recognizes the JSPS G8 Research Councils Initiative of Japan (DELTAS). Jeffrey Nittrouer recognizes the National Science Foundation of the U.S.A., grant EAR 1616747.

References

Alesheikh, A., Ghorbanali, A., Nouri, N., 2007. Coastline change detection using remote sensing. Int. J. Environ. Sci. Technol. 4, 61–66.
Bai, J., Xiao, R., Zhang, K., Gao, H., 2012. Arsenic and heavy metal pollution in wetland soils from tidal freshwater and salt marshes before and after the flow-sediment regulation regime in the Yellow River Delta, China. J. Hydrol. 450–451, 244–253.
Bi, N., Wang, H., Yang, Z., 2014a. Recent changes in the erosion-accretion patterns of the active Huanghe (Yellow River) delta lobe caused by human activities. Cont. Shelf Res. 90, 70–78.
Bi, N., Yang, Z., Wang, H., Xu, C., Guo, Z., 2014b. Impact of artificial water and sediment discharge regulation in the Huanghe (Yellow River) on the transport of particulate heavy metals to the sea. Catena 121, 232–240.
Chen, J., Zhou, W., Sun, P., 2009. Effects of water-sediment regulation by Xiaolangdi Reservoir on channel erosion in the lower Yellow River. J. Sediment. Res. 3, 1–7 (in Chinese with English abstract).
Chen, Z., Syvitski, J.P.M, Gao, S., Overeem, I., Kettner, A.J., 2012. Socio-economic impacts on flooding: a 4000 year history of the Yellow River, China. Ambio 41 (7), 682–698.
Chu, Z., Sun, X., Zhai, S., Xu, K., 2006. Changing pattern of accretion/erosion of the modem Yellow River (Huanghe) subaerial delta, China: based on remote sensing images. Mar. Geol. 227 (1), 13–30.
Dai, M., Yin, Z., Meng, F., Liu, Q., Cai, W., 2012. Spatial distribution of riverine DOC inputs to the ocean: an updated global synthesis. Curr. Opin. Environ. Sustain. 4, 170–178.
Deng, J., Zhuang, Z., 2001. The cause of recruitment variation of *Penaeus chinensis* in the Bohai Sea. J. Fish. Sci. China 7 (4), 125–128 (in Chinese with English abstract).
Ding, P., Wang, H., Meng, X., Zhu, J., 2013. Evolution and Cause Analysis of Typical Coastal Zones in China During the Last 50 years. Science Press, Beijing, pp. 6–21.
Dong, S.L., Zhang, S., Wang, F., 2002. Food sources and carbon budget of Chinese prawn *Penaeus chinensis*. Chin. J. Oceanol. Limnol. 20 (1), 32–40 (in Chinese with English abstract).
Dong, J., Xia, X., Wang, M., Lai, Y., Zhao, P., Dong, H., Zhao, Y., Wen, J., 2015. Effect of Water-Sediment Regulation of the Xiaolangdi Reservoir on the concentrations, bioavailability, and fluxes of PAHs in the middle and lower reaches of the Yellow River. J. Hydrol. 527, 101–112.
Giosan, L., Syvitski, J.P.M., Constantinescu, S., Day, J., 2014. Protect the world's deltas. Nature 516, 31–33.
Higgins, S., Overeem, Tanaka, A., Syvitski, J.P.M., 2013. Land subsidence at aquaculture facilities in the Yellow River delta, China. Geophys. Res. Lett. 40, 3898–3902.
Jin, X., 2001. The dynamics of major fishery resources in the Bohai Sea. J. Fish. Sci. China 7 (4), 22–26 (in Chinese with English abstract).
Li, Z., Wang, J., Zhao, Z., Zhou, J., Lv, Z., Dong, J., Liu, M., Jin, X., 2012. Resources enhancement of *Fenneropenaeus orientalis* in the Bohai Sea. Prog. Fish. Sci. 33 (3), 1–7 (in Chinese with English abstract).
Li, Q., Wang, Y., Bai, T., 2014. Review on water and sediment regulation of the Yellow River. J. Northwest A & F Univ. 42 (12), 227–234 (in Chinese with English abstract).
Lin, C., Su, J., Xu, B., Tang, Q., 2001. Long-term variations of temperature and salinity of the Bohai Sea and their influence on its ecosystem. Prog. Oceanogr. 49 (1–4), 7–19.
Liu, J.Y., 1990. Resource enhancement of Chinese shrimp, *Penaeus orientalis*. Bull. Mar. Sci. 47 (1), 124–133.
Liu, S.M., 2015. Response of nutrient transports to water–sediment regulation events in the Huanghe basin and its impact on the biogeochemistry of the Bohai. J. Mar. Syst. 141, 59–70.
Liu, S.M., Li, L.W., Zhang, G.L., Liu, Z., Yu, Z., Ren, J.L., 2012. Impacts of human activities on nutrient transports in the Huanghe (Yellow River) Estuary. J. Hydrol. 430–431, 103–110.
Meade, R.H., Parker, R., 1985. Sediments in rivers of the United States, in National Water Summary 1984. U. S. Geol. Surv. Water Supply Pap. 2275, 49–60.
Meybeck, M., Vörösmarty, C., 2005. Fluvial filtering of land-to-ocean fluxes: from natural Holocene variations to Anthropocene. Compt. Rendus Geosci. 337, 107–123.
Milliman, J.D., Meade, R.H., 1983. World-wide delivery of river sediment to the oceans. J. Geol. 91, 1–21.
Milliman, J.D., Syvitski, J.P.M., 1992. Geomorphic/tectonic control of sediment

discharge to the ocean: the importance of small mountainous rivers. J. Geol. 100, 525–544.
Nilsson, C., Reidy, C.A., Dynesius, M., Revenga, C., 2005. Fragmentation and flow regulation of the world's large river systems. Science 308, 405–408.
Pan, G., Krom, M.D., Zhang, M., Zhang, X., Wang, L., Dai, L., Sheng, Y., Mortimer, R.J.G., 2013. Impact of suspended inorganic particles on phosphorus cycling in the Yellow River (China). Environ. Sci. Technol. 47, 9685–9692.
Saito, Y., Wei, H., Zhou, Y., Nishimura, A., Sato, Y., Yokota, S., 2000. Delta progradation and chenier formation in the Huanghe (Yellow River) Delta, China. J. Asian Earth Sci. 18, 489–497.
Saito, Y., Yang, Z., Hori, K., 2001. The Huanghe (Yellow River) and Changjiang (Yangtze River) deltas: a review on their characteristics, evolution and sediment discharge during the Holocene. Geomorphology 41, 219–231.
Schwarz, H.E., Emel, J., Dickens, W.J., Rogers, P., Thompson, J., 1991. Water quality and flows. In: Turner, B.L., Clark, W.C., Kates, R.W., Richards, J.F., Matthews, J.T., Meyer, W.B. (Eds.), The Earth as Transferred by Human Actions. Cambridge University Press, Cambridge, pp. 253–270.
Seitzinger, S.P., Harrison, J.A., Dumont, E., Beusen, A.H.W., Bouwman, A.F., 2005. Sources and delivery of carbon, nitrogen, and phosphorus to the coastal zone: an overview of Global Nutrient Export from Watersheds (NEWS) models and their application. Glob. Biogeochem. Cycles 19, GB4S01.
Shang, H.X., Sun, Z.Y., Tian, S.M., 2015. Scouring and siltation characteristics in the lower Yellow River since 2000. The Yellow River 37 (8), 7–12 (in Chinese with English abstract).
Stanley, D.J., Warne, A.G., 1998. Nile delta in its destruction phase. J. Coast. Res. 14, 794–825.
Steffen, W., Sanderson, R.A., Tyson, P.D., Jäger, J., Matson, P.A., Moore III, B., Oldfield, F., Richardson, K., Schellnhuber, H.J., Turner, B.L., Wasson, R.J., 2004. Global Change and the Earth System: A Planet Under Pressure. Springer-Verlag, New York.
Sun, T., Yang, Z., 2010. Numerical modeling of the salinity distribution and environmental flows assessment in the Yellow River Estuary, China. In: Swayne, D.A., Yang, W., Voinov, A.A., Rizzoli, A., Filatova, T. (Eds.), Proceedings. Modelling for Environment's Sake, International Environmental Modelling and Software Society (iEMSs), 2010 International Congress on Environmental Modelling and Software, Ottawa, Canada.
Syvitski, J.P.M., 2012. Anthropocene: an epoch of our making. Glob. Chang. Newslett. 78, 12–15.
Syvitski, J.P.M., Kettner, A., 2007. On the flux of water and sediment into the Northern Adriatic. Cont. Shelf Res. 27, 296–308.
Syvitski, J.P.M., Kettner, A., 2011. Sediment flux and the Anthropocene. Phil. Trans. R. Soc. A 369, 957–975.
Syvitski, J.P.M., Saito, Y., 2007. Morphodynamics of deltas under the influence of humans. Glob. Planet. Chang. 57, 261–282.
Syvitski, J.P.M., Vörösmarty, C.J., Kettner, A.J., Green, P., 2005. Impact of humans on the flux of terrestrial sediment to the global coastal ocean. Science 308, 376–380.
Syvitski, J.P.M., Kettner, A.J., Overeem, I., Hutton, E.W.H., Hannon, M., Brakenridge, R., Day, J., Vörösmarty, C., Saito, Y., Giosan, L., Nicholls, R.J., 2009. Sinking deltas due to human activities. Nat. Geosci. 2, 681–686.
Tao, S., Eglinton, T., Montlucon, D., McIntyre, C., Zhao, M., 2015. Pre-aged soil organic carbon as a major component of the Yellow River suspended load: regional significance and global relevance. Earth Planet. Sci. Lett. 414, 77–86.
Tessler, Z.D., Vörösmarty, C.J., Grossberg, M., Gladkova, I., Aizenman, H., Syvitski, J.P.M., Foufoula-Georgiou, E., 2015. Profiling risk and sustainability in coastal deltas of the world. Science 349, 638–643.
Walling, D.E., Fang, D., 2003. Recent trends in the suspended sediment loads of the world's rivers. Glob. Planet. Chang. 39, 111–126.
Wan, Z., Luo, Q., Yan, Z., Liang, Y., 2013. Study on regulation index and operation mode of the Yellow River water and sediment regulation. The Yellow River 35 (5), 1–4 (in Chinese with English abstract).
Wang, H., Yang, Z., Bi, N., Li, H., 2005. Rapid shifts of the river plume pathway off the Huanghe (Yellow) River mouth in response to Water–Sediment Regulation Scheme in 2005. Chin. Sci. Bull. 50 (24), 2878–2884.
Wang, H., Yang, Z.S., Saito, Y., Liu, J.P., Sun, X., 2006a. Interannual and seasonal variation of the Huanghe (Yellow River) water discharge over the past 50 years: connections to impacts from ENSO events and dams. Glob. Planet. Chang. 50 (3–4), 212–225.
Wang, H., Yang, Z., Li, G., Jiang, W., 2006b. Wave climate modeling on the abandoned Huanghe (Yellow River) delta lobe and related deltaic erosion. J. Coast. Res. 22 (4), 906–918.
Wang, H., Yang, Z.S., Saito, Y., Liu, J.P., Sun, X., Wang, Y., 2007. Stepwise decreases of the Huanghe (Yellow River) sediment load (1950–2005): impacts of climate changes and human activities. Glob. Planet. Chang. 57 (3–4), 331–354.
Wang, H., Bi, N., Saito, Y., Wang, Y., Sun, X., Zhang, J., 2010a. Recent changes in sediment delivery by the Huanghe (Yellow River) to the sea: causes and environmental implications in its estuary. J. Hydrol. 39 (3–4), 302–313.
Wang, H., Bi, N., Wang, Y., Saito, Y., Yang, Z., 2010b. Tide-modulated hyperpycnal flows off the Huanghe (Yellow River) Mouth, China. Earth Surf. Process. Landf. 35 (11), 1315–1329.
Wang, H., Saito, Y., Bi, N., Sun, X., Yang, Z., 2011a. Recent changes of sediment flux to the western Pacific Ocean from major rivers in East and Southeast Asia. Earth Sci. Rev. 108 (1–2), 80–100.
Wang, Y., Liu, Z., Gao, H., Ju, L., Guo, X., 2011b. Response of salinity distribution around the Yellow River mouth to abrupt changes in river discharge. Cont. Shelf Res. 31, 685–694.
Wang, Y., Wang, H., Bi, N., Yang, Z., 2011c. Numerical modeling of hyperpycnal flows in an idealized river mouth. Estuar. Coast. Shelf Sci. 93 (3), 228–238.
Wang, X., Ma, H., Li, R., Song, Z., Wu, J., 2012. Seasonal fluxes and source variation of organic carbon transported by two major Chinese Rivers: the Yellow River and Changjiang (Yangtze) River. Glob. Biogeochem. Cycles 26, GB2025.
Wang, H., Yang, Z., Bi, N., 2014a. Changjiang (Yangtze) and Huanghe (Yellow) Rivers: historical reconstruction of land-use change and sediment load to the sea. In: Bianchi, T., Allison, M., Cai, W. (Eds.), Biogeochemical Dynamics at Major River-Coast Interfaces: Linkage With Global Change. Cambridge University Press, New York, pp. 118–137.
Wang, H., Wang, A., Bi, N., Zeng, X., Xiao, H., 2014b. Seasonal distribution of suspended sediment in the Bohai Sea, China. Cont. Shelf Res. 90, 17–32.
Wei, J., Chen, H., Liu, Y., Shan, K., Yao, Q., He, H., Yu, Z., 2011. Phosphorus forms of the suspended particulate matter in the Yellow River downstream during Water and Sediment Regulation 2008. Environ. Sci. 32 (2), 368–374 (in Chinese with English abstract).
Wu, X., Bi, N., Yuan, P., Li, S., Wang, H., 2015a. Sediment dispersal and accumulation off the present Huanghe (Yellow River) delta as impacted by the Water-Sediment Regulation Scheme. Cont. Shelf Res. 111, 126–138.
Wu, X., Bi, N., Kanai, Y., Saito, Y., Zhang, Y., Yang, Z., Fan, D., Wang, H., 2015b. Sedimentary records off the modern Huanghe (Yellow River) delta and their response to deltaic river channel shifts over the last 200 years. J. Asian Earth Sci. 108, 68–80.
Wu, X., Bi, N., Xu, J.P., Nittrouer, J., Yang, Z., Saito, Y., Wang, H., 2017. Stepwise morphological evolution of the active Yellow River (Huanghe) delta lobe (1976–2013): dominant roles of riverine discharge and sediment grain size. Geomorphology 292, 115–127.
Xu, J., 2003. Sediment flux into the sea as influenced by the changing human activities and precipitation: example of the Huanghe River, China. Acta Oceanol. Sin. 25 (5), 125–135.
Yang, S.L., Milliman, J.D., Li, P., Xu, K., 2011a. 50,000 dams later: erosion of the Yangtze River and its delta. Glob. Planet. Chang. 75 (1–2), 14–20.
Yang, Z.S., Ji, Y., Bi, N., Lei, K., Wang, H., 2011b. Sediment transport off the Huanghe (Yellow River) delta and in the adjacent Bohai Sea in winter and seasonal comparison. Estuar. Coast. Shelf Sci. 93 (3), 173–182.
Yang, S.L., Milliman, J.D., Xu, K.H., Deng, B., Zhang, X.Y., Luo, X.X., 2014. Downstream sedimentary and geomorphic impacts of the Three Gorges Dam on the Yangtze River. Earth Sci. Rev. 138, 469–486.
Yang, S.L., Xu, K.H., Milliman, J.D., Yang, H.F., Wu, C.S., 2015. Decline of Yangtze River water and sediment discharge: impact from natural and anthropogenic changes. Sci Rep 5, 12581.
Zhang, L., Wang, L., Cai, W., Liu, D., Yu, Z., 2013. Impact of human activities on organic carbon transport in the Yellow River. Biogeosciences 10, 2513–2524.
Zhang, J., Huang, H., Bi, H., 2015. Land subsidence in the modern Yellow River Delta based on InSAR time series analysis. Nat. Hazards 75, 2385–2397.